IMMUNODEFICIENCY



# Multiomics dissection of human RAG deficiency reveals distinctive patterns of immune dysregulation but a common inflammatory signature

Marita Bosticardo[1]†, Kerry Dobbs[1]†, Ottavia M. Delmonte[1]†, Andrew J. Martins[2]‡, Francesca Pala[1], Tomoki Kawai[1]§, Heather Kenney[1], Gloria Magro[1], Lindsey B. Rosen[1], Yasuhiro Yamazaki[1], Hsin-Hui Yu[1,3], Enrica Calzoni[1], Yu Nee Lee[4], Can Liu[2]‡, Jennifer Stoddard[5], Julie Niemela[5], Danielle Fink[6], Riccardo Castagnoli[1]¶, Meredith Ramba[7], Aristine Cheng[1]#, Deanna Riley[8], Vasileios Oikonomou[1], Elana Shaw[1], Brahim Belaid[9], Sevgi Keles[10], Waleed Al-Herz[11,12], Caterina Cancrini[13,14], Cristina Cifaldi[13], Safa Baris[15,16], Svetlana Sharapova[17], Catharina Schuetz[18], Andrew R. Gennery[19], Alexandra F. Freeman[1], Raz Somech[4], Sharon Choo[20], Silvia C. Giliani[21,22,23], Tayfun Güngör[24,25], Daniel Drozdov[24,25,26], Isabelle Meyts[27,28], Despina Moshous[29,30], Benedicte Neven[29,30], Roshini S. Abraham[31], Aisha El-Marsafy[32], Maria Kanariou[33], Alejandra King[34], Francesco Licciardi[35], Mario E. Cruz-Muñoz[36], Paolo Palma[13,37], Cecilia Poli[38], Mehdi Adeli[39], Mattia Algeri[40,41]**, Fayhan J. Alroqi[42], Paul Bastard[43,44], Jenna R. E. Bergerson[1], Claire Booth[45], Ana Brett[46,47], Siobhan O. Burns[48,49], Manish J. Butte[50], Nurcicek Padem[51], M. Teresa de la Morena[52], Ghassan Dbaibo[53,54], Suk See de Ravin[1], Dimana Dimitrova[55], Reda Djidjik[9], Mayra B. Dorna[56], Cullen M. Dutmer[57], Reem Elfeky[58], Fabio Facchetti[59], Ramsay L. Fuleihan[60], Raif S. Geha[61], Luis I. Gonzalez-Granado[62,63,64], Liis Haljasmägi[65], Hanadys Ale[66,67], Anthony Hayward[68], Anna M. Hifanova[69], Winnie Ip[45], Blanka Kaplan[70,71], Neena Kapoor[72], Elif Karakoc-Aydiner[15,16], Jaanika Kärner[65], Michael D. Keller[73], Blachy J. Dávila Saldaña[73]††, Ayça Kiykim[74], Taco W. Kuijpers[75], Elena E. Kuznetsova[76], Elena A. Latysheva[77], Jennifer W. Leiding[78,79,80], Franco Locatelli[40,41], Guisela Alva-Lozada[81], Christine McCusker[82], Fatih Celmeli[83], Megan Morsheimer[84], Ahmet Ozen[15,16], Nima Parvaneh[85], Srdjan Pasic[86], Alessandro Plebani[87], Kahn Preece[88], Susan Prockop[89], Inga S. Sakovich[17], Elena E. Starkova[90], Troy Torgerson[91], James Verbsky[92], Jolan E. Walter[93], Brant Ward[94]‡‡, Elizabeth L. Wisner[95], Deborah Draper[1], Katherine Myint-Hpu[1], Pooi M. Truong[1], Michail S. Lionakis[1], Morgan B. Similuk[96], Centralized Sequencing Program Group§§, Magdalena A. Walkiewicz[96], Amy Klion[97], Steven M. Holland[1], Cihan Oguz[98], Dusan Bogunovic[99], Kai Kisand[65], Helen C. Su[1,100], John S. Tsang[2]‡, Douglas Kuhns[6], Anna Villa[101,102], Sergio D. Rosenzweig[5], Stefania Pittaluga[8], Luigi D. Notarangelo[1]*

**Human recombination-activating gene (RAG) deficiency can manifest with distinct clinical and immunological phenotypes. By applying a multiomics approach to a large group of *RAG*-mutated patients, we aimed at characterizing the immunopathology associated with each phenotype. Although defective T and B cell development is common to all phenotypes, patients with hypomorphic *RAG* variants can generate T and B cells with signatures of immune dysregulation and produce autoantibodies to a broad range of self-antigens, including type I interferons. T helper 2 ($T_H2$) cell skewing and a prominent inflammatory signature characterize Omenn syndrome, whereas more hypomorphic forms of RAG deficiency are associated with a type 1 immune profile both in blood and tissues. We used cellular indexing of transcriptomes and epitopes by sequencing (CITE-seq) analysis to define the cell lineage–specific contribution to the immunopathology of the distinct RAG phenotypes. These insights may help improve the diagnosis and clinical management of the various forms of the disease.**

## INTRODUCTION

The recombination-activating gene (RAG) proteins RAG1 and RAG2 initiate the process of V(D)J recombination, allowing the development of mature T and B cells and effective adaptive immune responses (*1*). Biallelic loss-of-function mutations in *RAG1* or *RAG2* cause early arrest of T and B cell development, leading to $T^-$ $B^-$ severe combined immune deficiency disease (SCID) (*2*). Hypomorphic variants in the *RAG* genes are linked to a spectrum of phenotypes, including Omenn syndrome (OS), leaky SCID (LS), and delayed-onset combined immune deficiency (CID) (*3*–*5*). Each phenotype has distinctive features. OS is defined by early-onset generalized skin rash, eosinophilia, elevated immunoglobulin E (IgE), and autologous, oligoclonal T cells infiltrating skin and various organs. LS is often diagnosed in early childhood with autoimmune cytopenias and increased γδ T cell receptor (TCRγδ) T cells (*6*, *7*). CID is typically diagnosed later in life and is frequently marked by the presence of granulomas and autoimmunity (*8*). Excellent survival (~90%) has been reported after hematopoietic stem cell transplantation (HSCT) in patients with positive newborn

[1]Laboratory of Clinical Immunology and Microbiology, National Institute of Allergy and Infectious Diseases, National Institutes of Health, Bethesda, MD, USA. [2]Multiscale Systems Biology Section, Laboratory of Immune System Biology, NIAID, NIH, Bethesda, MD, USA. [3]Department of Pediatrics, National Taiwan University Children's Hospital, Taipei, Taiwan. [4]Pediatric Department A and the Immunology Service, Jeffrey Modell Foundation Center, Edmond and Lily Safra Children's Hospital, Sheba Medical Center, 52621 Tel HaShomer, Israel. [5]Immunology Service, Department of Laboratory Medicine, National Institutes of Health Clinical Center, Bethesda, MD, USA. [6]Neutrophil Monitoring Laboratory, Leidos Biomedical Research Inc., Frederick National Laboratory for Cancer Research, Frederick, MD, USA. [7]Precision Immunology Institute, Icahn School of Medicine at Mount Sinai, New York City, NY, USA. [8]Laboratory of Pathology, National Cancer Institute, National Institutes of Health, Bethesda, MD, USA. [9]Department of Medical Immunology, Beni Messous University Hospital Center, Faculty of Pharmacy, University of Algiers, Algiers, Algeria. [10]Division of Pediatric Allergy and Immunology, Meram Faculty of Medicine, Necmettin Erbakan University, Konya, Turkey. [11]Department of Pediatrics, College of Medicine, Kuwait University, Safat, Kuwait City, Kuwait. [12]Allergy and Clinical Immunology Unit, Pediatric Department, Al-Sabah Hospital, Kuwait City, Kuwait. [13]Department of Systems Medicine, University of Rome Tor Vergata, Rome, Italy. [14]Research Unit of Primary Immunodeficiencies, Academic Department of Pediatrics, Bambino Gesu' Children's Hospital, Scientific Institute for Research and Heathcare (IRCCS), Rome, Italy. [15]Faculty of Medicine, Division of Pediatric Allergy and Immunology, Marmara University, Istanbul, Turkey. [16]Isil Berat Barlan Center for Translational Medicine, Istanbul Jeffrey Modell Foundation Diagnostic Center for Primary Immune Deficiencies, Istanbul, Turkey. [17]Belarusian Research Center for Pediatric Oncology, Hematology and Immunology, Minsk, Belarus. [18]Department of Paediatrics, Universitätsklinikum Carl Gustav Carus, Technische Universität Dresden, Dresden, Germany. [19]Translational and Clinical Research Institute, Newcastle University, Newcastle upon Tyne, UK. [20]Department of Allergy and Immunology, Royal Children's Hospital, Melbourne, VIC, Australia. [21]Angelo Nocivelli Institute for Molecular Medicine, Department of Molecular and Translational Medicine, University of Brescia, Brescia, Italy. [22]Laboratory Department, Spedali Civili, Brescia, Italy. [23]National Center for Gene Therapy and Drugs based on RNA Technology, CN3, Brescia, Italy. [24]Division of Hematology/Oncology/Immunology, Gene-Therapy, and Stem Cell Transplantation, University Children's Hospital Zürich, Zürich, Switzerland. [25]Eleonore Foundation & Children's Research Center (CRC), Zürich, Switzerland. [26]Division of Pediatric Hematology and Oncology, Department of Pediatrics, Kantonsspital Aarau, Aarau, Switzerland. [27]Department of Immunology and Microbiology, Inborn Errors of Immunity, KU Leuven, Leuven, Belgium. [28]University Hospitals Leuven and ERN-RITA Core Center, Leuven, Belgium. [29]Hôpital Necker Enfants Malades, Assistance Publique-Hôpitaux de Paris, Université Paris Cité, Paris, France. [30]Institut Imagine, Université Paris Cité, Paris, France. [31]Department of Pathology and Laboratory Medicine, Nationwide Children's Hospital, Columbus, OH, USA. [32]Department of Pediatrics, Faculty of Medicine, Cairo University, Cairo, Egypt. [33]Department of Immunology—Histocompatibility, Specialized & Referral Center for Primary Immunodeficiencies—Paediatric Immunology, "Aghia Sophia" Children's Hospital, Athens, Greece. [34]Departamento de Pediatría, Hospital Luis Calvo Mackenna, Santiago, Chile. [35]Immuno-reumatologia, Pediatria Specialistica Universitaria, Ospedale Infantile Regina Margherita, Torino, Italy. [36]Facultad de Medicina, Universidad Autónoma del Estado de Morelos, Cuernavaca, Morelos, Mexico. [37]Clinical Immunology and Vaccinology Unit, Children's Hospital "Bambino Gesu," Rome, Italy. [38]Faculty of Medicine, Clínica Alemana Universidad del Desarrollo Roberto del Rio, Santiago, Chile. [39]Department of Immunology, Sidra Medicine, Ar-Rayyan, Qatar. [40]Department of Hematology/Oncology, Cell and Gene Therapy, IRCCS Bambino Gesù Children's Hospital, Rome, Italy. [41]Catholic University of the Sacred Heart, Rome, Italy. [42]King Abdullah International Medical Research Center, King Saud bin Abdulaziz University for Health Sciences, Riyadh, Saudi Arabia. [43]Pediatric Hematology-Immunology and Rheumatology Unit, Necker Hospital for Sick Children, Assistance Publique-Hôpitaux de Paris (AP-HP), Paris, France. [44]Laboratory of Human Genetics of Infectious Diseases, Necker Branch, INSERM U1163, Necker Hospital for Sick Children, Paris, France. [45]Molecular and Cellular Immunology, UCL Great Ormond Street Institute of Child Health, London, UK. [46]Hospital Pediátrico, Unidade Local de Saúde de Coimbra, Coimbra, Portugal. [47]Clínica Universitária de Pediatria, Faculdade de Medicina, Universidade de Coimbra, Coimbra, Portugal. [48]Institute of Immunity and Transplantation, University College London, London, UK. [49]Department of Immunology, Royal Free London NHS Foundation Trust, London, UK. [50]Department of Pediatrics, Division of Immunology, Allergy, and Rheumatology, University of California, Los Angeles, Los Angeles, CA, USA. [51]Division of Pediatric Pulmonology, Allergy-Immunology and Sleep Medicine, Riley Hospital for Children/Indiana University, Indianapolis, IN, USA. [52]Division of Immunology, Department of Pediatrics, Seattle Children's Hospital, University of Washington, Seattle, WA, USA. [53]Department of Pediatrics and Adolescent Medicine, Faculty of Medicine, American University of Beirut Medical Center, Beirut, Lebanon. [54]Center for Infectious Diseases Research (CIDR) and WHO Collaborating Center for Reference and Research on Bacterial Pathogens, American University of Beirut, Beirut, Lebanon. [55]Experimental Transplantation and Immunotherapy Branch, National Cancer Institute, National Institutes of Health, Bethesda, MD, USA. [56]Division of Allergy and Immunology, Department of Pediatrics, Faculdade de Medicina da Universidade de São Paulo, São Paulo, Brazil. [57]Allergy and Immunology Section, Children's Hospital Colorado and University of Colorado School of Medicine, Aurora, CO, USA. [58]Department of Clinical Immunology, Royal Free Hospital, London, UK. [59]Section of Pathology, Department of Molecular and Translational Medicine, University of Brescia, Spedali Civili di Brescia, Brescia, Italy. [60]Division of Allergy & Immunology, Columbia University Irving Medical Center, New York, NY, USA. [61]Division of Immunology, Boston Children's Hospital, Boston, MA, USA. [62]Primary Immunodeficiency Unit, Pediatrics, Hospital 12 Octubre, Madrid, Spain. [63]Instituto de Investigation Hospital 12 Octubre (imas12), Madrid, Spain. [64]School of Medicine Complutense University, Madrid, Spain. [65]Institute of Biomedicine and Translational Medicine, University of Tartu, Tartu, Estonia. [66]Division of Immunology, Allergy and Rheumatology, Joe DiMaggio Children's Hospital, Memorial Healthcare System, Hollywood, FL, USA. [67]Florida International University Herbert Wertheim College of Medicine, Miami, FL, USA. [68]Division of Infectious Diseases, Department of Pediatrics, Brown University and Rhode Island Hospital, Providence, RI, USA. [69]Department of Pediatric Infectious Diseases and Pediatric Immunology, Shupyk National Healthcare University of Ukraine, Kiev, Ukraine. [70]Division of Allergy, Asthma and Immunology, Cohen Children's Medical Center, Northwell Health, New Hyde Park, NY, USA. [71]Donald and Barbara Zucker School of Medicine at Hofstra/Northwell, Hempstead, NY, USA. [72]Children's Hospital of Los Angeles, Los Angeles, CA, USA. [73]Division of Allergy and Immunology, Children's National Hospital, Washington, DC, USA. [74]Division of Pediatric Allergy and Immunology, Cerrahpasa Faculty of Medicine, Istanbul University-Cerrahpasa, Istanbul, Turkey. [75]Department of Pediatric Immunology, Amsterdam UMC Locatie AMC, Amsterdam, Netherlands. [76]Hematology Department, Regional Clinical Hospital, Orenburg, Russia. [77]Immunopathology Department, NRC Institute of Immunology FMBA, Pigorov Russian National Research Medical University, Moscow, Russia. [78]Division of Allergy and Immunology, Department of Pediatrics, Johns Hopkins University, Baltimore, MD, USA. [79]Institute for Clinical and Translational Research, Johns Hopkins All Children's Hospital, St. Petersburg, FL, USA. [80]Cancer and Blood Disorders Institute, Johns Hopkins All Children's Hospital, St. Petersburg, FL, USA. [81]Allergy and Immunology Division Hospital Nacional Edgardo Rebagliati Martins, Lima, Peru. [82]Division of Allergy and Clinical Immunology, Department of Pediatrics, Montreal Children's Hospital, McGill University Health Centre, Montreal, QC, Canada. [83]Immunology and Allergy Diseases, Saglık Bilimleri University, Antalya Training and Research Hospital Pediatric, Antalya, Turkey. [84]Division of Allergy, Immunology and Transplantation, National Institutes of Allergy and Infectious Diseases, National Institutes of Health, Bethesda, MD, USA. [85]Infectious Disease Research Center, Tehran University of Medical Sciences, Tehran, Iran. [86]Department of Pediatric Immunology, Mother and Child Health Institute, Medical Faculty, University of Belgrade, Belgrade, Serbia. [87]University of Brescia, Brescia, Italy. [88]Department of Immunology, John Hunter Children's Hospital, Newcastle, NSW, Australia. [89]Dana-Farber/Boston Children's Cancer and Blood Disorders Center, Boston, MA, USA. [90]Clinical Department, Regional Clinical Hospital No. 2, Orenburg, Russia. [91]Allen Institute for Immunology, Seattle, WA, USA. [92]Division of Rheumatology, Department of Pediatrics, Medical College of Wisconsin and Children's Wisconsin, Milwaukee, WI, USA. [93]Division of Pediatric Allergy/Immunology, University of South Florida at Johns Hopkins All Children's Hospital, St. Petersburg, FL, USA. [94]Division of Rheumatology, Allergy and Immunology, Virginia Commonwealth University, Richmond, VA, USA. [95]Division of Allergy Immunology, Department of Pediatrics, Louisiana State University Health Sciences Center New Orleans, New Orleans, LA, USA. [96]Division of Intramural Research, National Institute of Allergy and Infectious Diseases, National Institutes of Health, Bethesda, MD, USA. [97]Laboratory of Parasitic Diseases, NIAID, NIH, Bethesda, MD, USA. [98]Integrated Data Sciences Section, Research Technologies Branch, National Institute of Allergy and Infectious Diseases, National Institutes of Health, Bethesda, MD, USA. [99]Center for Genetic Errors of Immunity, Columbia University Medical Center, New York City, NY, USA. [100]Department of Pathology and Laboratory Medicine, Perelman School of Medicine, University of Pennsylvania, Philadelphia, PA, USA. [101]Milan Unit, Istituto di Ricerca Genetica e Biomedica, Consiglio Nazionale delle Ricerche, Milan, Italy. [102]San Raffaele-Telethon Institute for Gene Therapy (SR-Tiget), IRCSS San Raffaele Scientific Institute, Milan 20132, Italy.

*Corresponding author. Email: luigi.notarangelo2@nih.gov

†These authors contributed equally to this work.

‡Present address: Center for Systems and Engineering Immunology, Yale University School of Medicine, New Haven, CT, USA; Department of Immunobiology, Yale University School of Medicine, New Haven, CT, USA; Department of Biomedical Engineering, Yale University, New Haven, CT, USA.

§Present address: Shizuoka Children's Hospital, Department of Allergy and Clinical Immunology, Shizuoka, Japan.

¶Present address: Pediatric Unit, Department of Clinical, Surgical, Diagnostic, and Pediatric Sciences, University of Pavia, Pavia, Italy; Pediatric Clinic, Fondazione IRCCS Policlinico San Matteo, Pavia, Italy.

#Present address: Department of Medicine, National Taiwan University Hospital and National Taiwan University College of Medicine, Taipei, Taiwan.

**Present address: Department of Hematology/Oncology, Cell and Gene Therapy, IRCCS Bambino Gesù Children's Hospital, Rome, Italy; Department of Health Sciences, Magna Graecia University, Catanzaro, Italy.

††Present address: University of Cincinnati School of Medicine and Cincinnati Children's Hospital Medical Center, Cincinnati, OH, USA.
‡‡Present address: Division of Allergy and Immunology, Children's National Hospital, Washington, DC, USA; Department of Pediatrics, George Washington University School of Medicine and Health Sciences, Washington, DC, USA.
§§Individuals in the Centralized Sequencing Program Group and their affiliations are listed after the Acknowledgments.

screening (*9*). However, delayed diagnosis and chronic organ damage reduce survival after HSCT in patients with CID (*10*).

We previously showed that the spectrum of RAG deficiency phenotypes correlates with recombination activity of the mutant RAG alleles, with minimal levels in patients with SCID and OS but residual functional activity in patients with LS and CID (*11*, *12*). However, this correlation does not provide mechanistic insights into the immunopathological signatures related to the various phenotypes. To address this, we applied a multiomics approach to characterizing the immunopathology of RAG deficiency in 157 patients spanning the disease spectrum.

## RESULTS

### Clinical and immunological phenotype of *RAG*-mutated patients

A history of infections was present in all patient groups with similar frequencies; skin rash and granulomas were typical of OS and CID, respectively, whereas cytopenias and other autoimmune manifestations were found to affect almost exclusively patients with CID and LS (Fig. 1A and data file S1). These manifestations of immune dysregulation required systemic immunosuppressants or immunomodulatory drugs in 75 of 157 patients before samples were collected. Systemic steroids were used in 58 patients, and cyclosporine A was required in 17 patients, most commonly in those with OS ($n = 15$). Among biologicals, rituximab was used in 11 patients. Serotherapy was used in eight patients, seven of whom had OS.

Severe T cell lymphopenia was observed in patients with SCID. The proportions of naïve $CD45RA^+$ CD4 T cells were markedly reduced in patients with OS but partially preserved in patients with LS and CID (fig. S1, A to E). Circulating B cells were markedly reduced or absent in patients with SCID and OS but were present, albeit at lower levels than normal, in patients with LS and CID (fig. S1F). Consistent with this, IgA and IgM serum levels were often normal in patients with LS and CID but absent in patients with SCID (fig. S1, G and H). Last, natural killer (NK) cells were present in normal numbers in all groups of patients (fig. S1I).

### Functional activity of *RAG* mutant alleles

Biallelic *RAG1* variants were identified in 121 patients (77.1% of the total), whereas 36 patients (22.9%) carried *RAG2* variants (data file S1). We identified 98 distinct variants in *RAG1* and 32 variants in *RAG2*, and using an in vitro recombination assay (*11*, *12*), we assessed the functional activity of 119 of them (data file S2). Upon evaluating the recombination activity associated with each mutant allele per patient, we found that patients with CID and LS carried *RAG* variants with residual recombination activity (means ± SEM, 30.27 ± 3.00 and 23.13 ± 3.90% of wild-type allele, respectively). By contrast, variants detected in patients with OS and SCID had almost null function (4.93 ± 1.58 and 4.17 ± 1.43%, respectively) (Fig. 1C and data file S3). This pattern was also observed when analyzing *RAG1* and *RAG2* variants separately (fig. S1J and data file S4).

### T cell and B cell development in *RAG*-mutated patients has common features, with leakier defects in LS and CID

We investigated in vitro T cell differentiation of $CD34^+$ cells from 13 *RAG*-mutated patients in an artificial thymic organoid (ATO) system (*13*). We observed that human *RAG* deficiency was permissive for the development of $CD4^+CD8^+$ double-positive (DP) cells but impaired the generation of $CD3^+TCR\alpha\beta^+$ (or $TCR\gamma\delta^+$) cells, regardless of the severity of the clinical phenotype (Fig. 2A), confirming our previous observation (*14*).

Hypomorphic *RAG* variants affect sequential rearrangements at the *TRA* locus, resulting in a lower frequency of rearrangements involving the 5′ *TRAV* and the 3′ *TRAJ* genes (*15*). Cells expressing Vα7.2 (the product of the 5′ *TRAV1-2* gene) represented 4.42 ± 2.37% (means ± SD) of circulating $CD3^+$ cells from healthy donors (HDs) but only 0.33 ± 0.76% of $CD3^+$ cells from *RAG*-mutated patients, irrespective of the clinical phenotype (Fig. 2B and data file S5). $V\alpha7.2^+$ cells comprised 2.37 ± 1.03% of $CD3^+$ cells in heterozygous relatives of RAG-affected patients, a frequency intermediate between what was detected in patients and HDs. Similar features were observed when analyzing the proportion of mucosal-associated invariant T (MAIT) cells, a subset of nonconventional T cells expressing the invariant *TRAV1-2* gene and CD161. MAIT cells represented 2.60 ± 2.27% of $CD3^+$ cells in HDs, but only 0.21 ± 0.35% in *RAG*-mutated patients and 1.09 ± 0.86% in heterozygous individuals (Fig. 2C and data file S5). Thus, hypomorphic *RAG* variants have profound effects on the composition of the T cell repertoire. Furthermore, RAG haploinsufficiency has a functional impact on the quality of V(D)J recombination.

Next, we analyzed B cell development in bone marrow aspirates from 18 *RAG*-mutated patients (11 CID, 2 LS, 3 OS, and 2 SCID) and 5 HDs. A significant enrichment in the proportion of pro-B and pre-B I cells—indicative of an early block in B cell development—was observed in most patients, irrespective of their clinical phenotype (Fig. 2, D and E; fig. S2, A and B; and data file S6). However, some leakiness of this defect was detected in patients with CID and LS, as indicated by the residual development of immature B cells and the accumulation of mature/recirculating B cells (Fig. 2F).

### Cutaneous and systemic inflammatory signatures of patients with OS and CID

Cutaneous manifestations with T cell infiltrates are a hallmark of RAG-associated OS and CID (*8*). CD4 and CD8 T cell infiltrates and abundances of *IFNG*, *CXCL9*, and *CXCL10* transcripts were detected in skin biopsies of patients with OS and CID who have granulomas (Fig. 3, A and B, and fig. S3). However, although expression of the transcription factor T-bet confirmed a prominent type 1 signature in granulomatous lesions of patients with CID, the T helper 2 ($T_H2$) cell–specific transcription factor GATA-binding factor 3 (GATA3) was abundantly expressed in skin infiltrates from patients with OS, along with more limited T-bet expression (Fig. 3, A and B). Eosinophilia and elevated serum IgE represent biomarkers of $T_H2$ skewing in OS (*8*) and were not observed in other RAG-associated phenotypes (Fig. 3, C and D, and data file S1). To further investigate

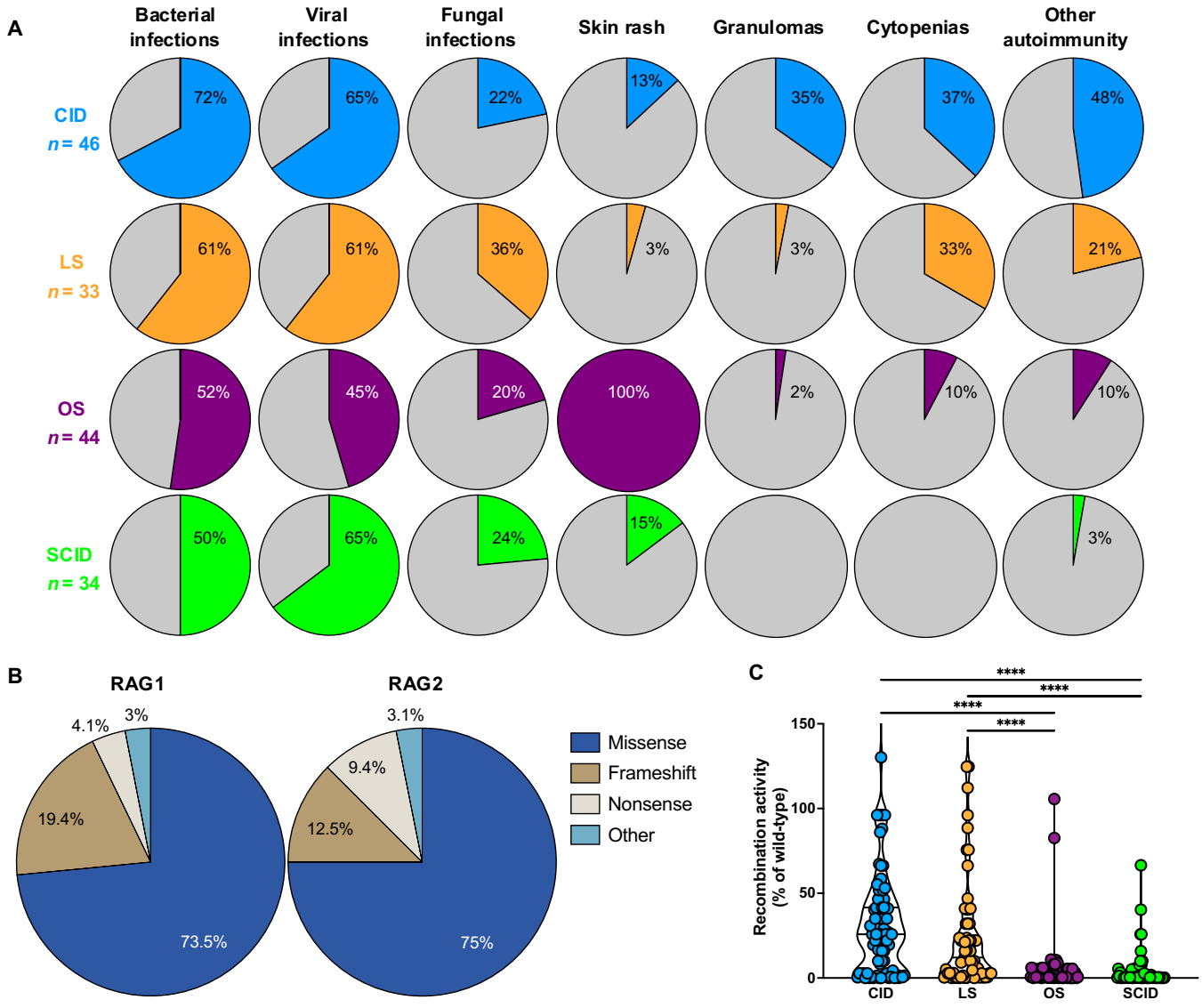


**Fig. 1. Clinical manifestations, type of mutations, and recombination activity in our cohort of *RAG*-mutated patients.** (**A**) Pie charts indicating the proportion of *RAG*-mutated patients in each of the groups (CID, LS, OS, and SCID) who suffered from bacterial, viral, and fungal infections, skin rash, granulomas, cytopenias, or other autoimmune manifestations. (**B**) Pie charts showing the proportion of missense, frameshift, nonsense, and insertion/deletion variants identified in *RAG1* (left) and *RAG2* (right) genes in our cohort of patients. (**C**) Recombination activity of individual mutant *RAG* variants, as compared with wild-type alleles. The variants are grouped on the basis of the clinical phenotype of the patients: CID ($n = 90$), LS ($n = 63$), OS ($n = 81$), and SCID ($n = 54$). Results are shown as violin scatter plots with median and quartile. Kruskal-Wallis *H* test, followed by Dunn's multiple comparisons test. ****$P < 0.0001$.

the mechanisms accounting for the $T_H2$ cutaneous phenotype of OS, we profiled circulating CD4 and CD8 memory T cells from *RAG*-mutated patients for the expression of the skin-homing receptor CD162, which binds P-selectin on the surface of endothelial cells to allow the transmigration of T cells to the skin (*16*). Patients with OS exhibited an increased frequency of circulating $CD162^+$ memory T cells (Fig. 3, E and F, and data file S7). Next, we investigated the distribution of circulating $T_H$ and T follicular helper ($T_{FH}$) cell subsets by analyzing surface expression of chemokine receptors (*17*). A markedly increased frequency of $T_H2$ cells was observed in patients with OS (Fig. 3G and data file S7), associated with higher proportions of circulating $T_{FH}2$ cells (Fig. 3H and data file S7) and lineage $(Lin)^-$ $CD127^+CD117^+CD294^+$ group 2 innate lymphoid cells (ILC2s) (Fig. 3I and data file S7). Thus, a prominent systemic "type 2" phenotype in the context of a broader inflammatory cutaneous response is a characteristic feature of OS.

## *RAG*-mutated patients exhibit a broad inflammatory signature

To better characterize the immune dysregulation associated with RAG deficiency, we quantified the concentration of 33 soluble biomarkers in the plasma of *RAG*-mutated patients and HDs. Significantly increased levels of a large number of these biomarkers were detected in *RAG*-mutated patients (Fig. 4A, fig. S4, and data file S8). OS emerged as the phenotype with the strongest systemic inflammatory signature (Fig. 4A). This included canonical type 2 immune

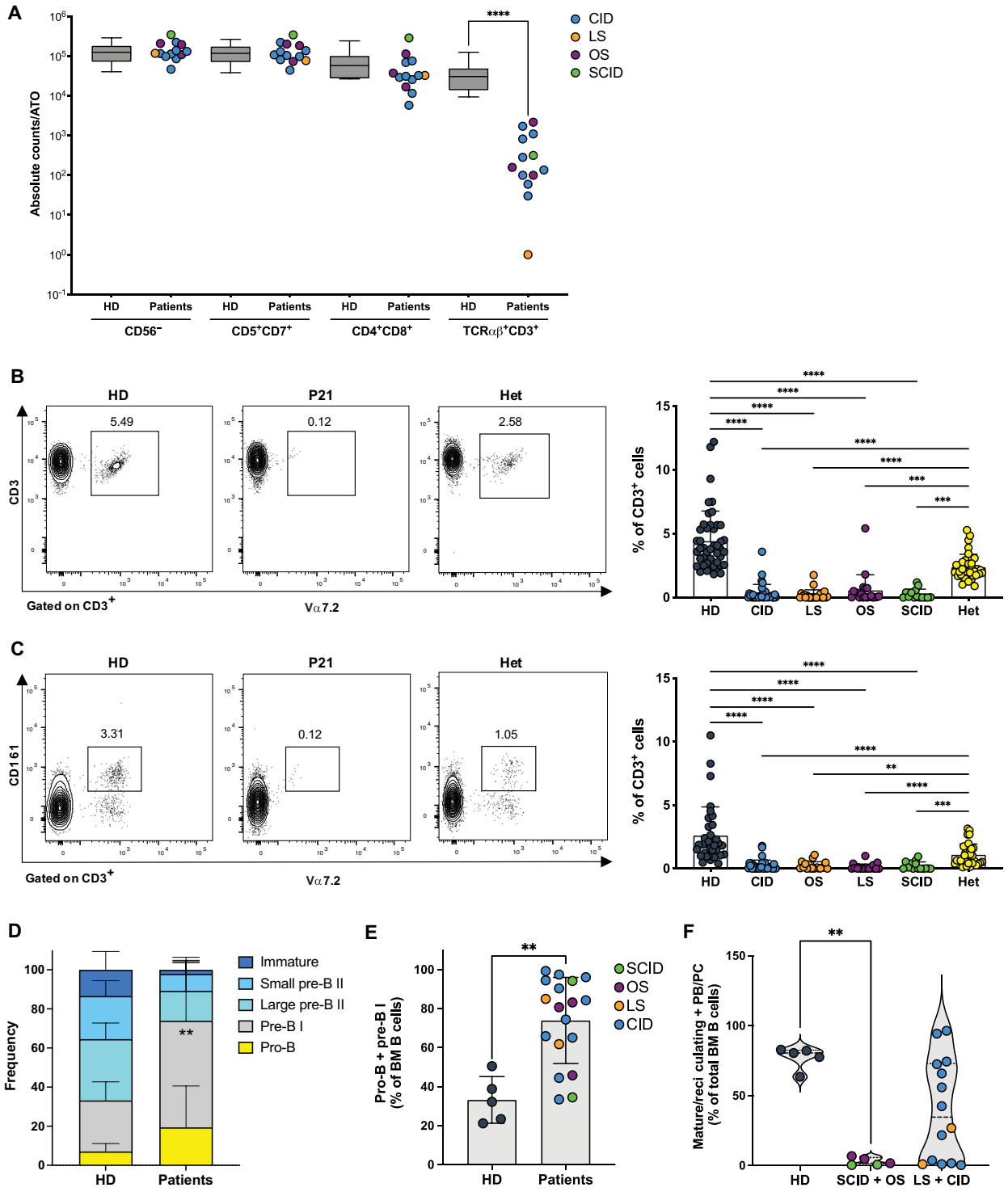


**Fig. 2. Analysis of in vitro T cell development, distal TCRVα gene rearrangement usage, and BM B cell development in *RAG*-mutated patients.** (**A**) Graph showing absolute cell counts of T cell subsets in the ATOs. Box-and-whisker plots show median and 5 to 95% confidence intervals for all HDs analyzed ($n = 11$). Each symbol represents a patient's sample (CID, $n = 8$; LS, $n = 1$; OS, $n = 3$; SCID, $n = 1$). (**B** and **C**) Representative flow cytometry plots and bar graphs showing the frequency of (B) $CD3^+TCRV\alpha7.2^+$ cells in HDs ($n = 45$), *RAG*-mutated patients (CID, $n = 35$; LS, $n = 23$; OS, $n = 20$; SCID, $n = 14$), and heterozygous individuals ($n = 34$) and (C) the frequency of $CD3^+TCRV\alpha7.2^+CD161^+$ MAIT cells in HDs ($n = 34$), *RAG*-mutated patients (CID, $n = 34$; LS, $n = 21$; OS, $n = 19$; SCID, $n = 14$), and heterozygous individuals ($n = 31$). (**D**) Stacked bar graph summarizing the frequency of bone marrow (BM) B cell subsets in HDs ($n = 5$) and *RAG*-mutated patients ($n = 17$). (**E**) Bar graph with scatter dot plots summarizing the frequency of the combined pro-B and pre-B I cell subsets in HDs ($n = 5$) and *RAG*-mutated patients ($n = 17$). Bars [(B) to (E)] show mean values ± SD. (**F**) Violin plots with scatter dot plots showing the frequency of mature/recirculating B and plasmablasts/plasma cells (PB/PC) among total BM B cells in HDs ($n = 5$) and patients with SCID + OS ($n = 5$) and LS + CID ($n = 12$). Violin plots show median and quartiles. In all panels, data from individual experiments were pooled. Data were analyzed using [(A), (D), and (E)] Mann-Whitney *U* test, two-tailed, or [(B), (C), and (F)] Kruskal-Wallis *H* test, followed by Dunn's multiple comparisons test. $^{**}P < 0.005$, $^{***}P < 0.001$, and $^{****}P < 0.0001$.

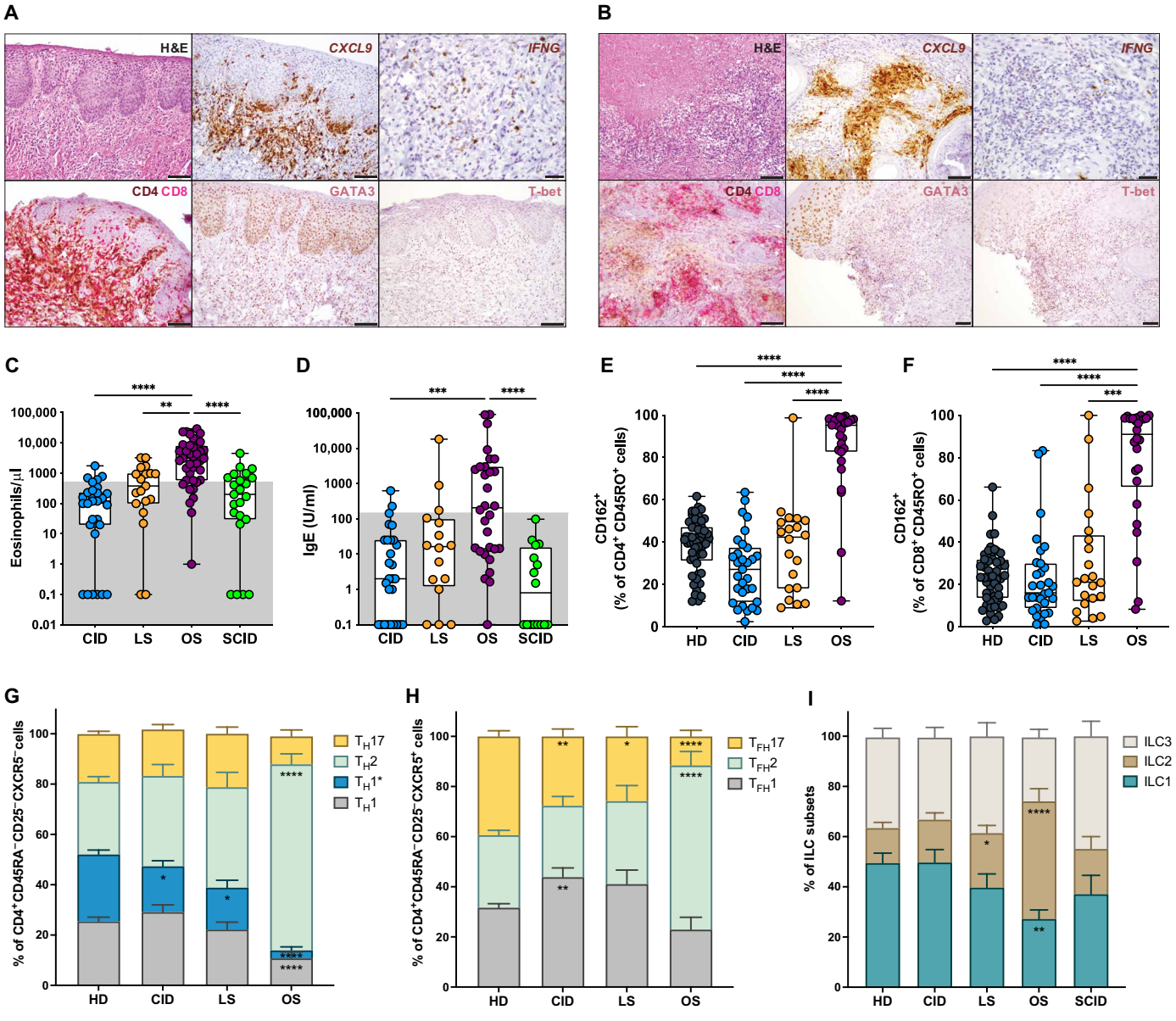


**Fig. 3. Inflammatory profile in skin lesions of patients with OS and CID and distribution of $T_H$ cell, $T_{FH}$ cell, and ILC subsets in *RAG*-mutated patients.** (**A** and **B**) Representative [hematoxylin and eosin (H&E), CD4/CD8, GATA3, and T-bet] and RNAscope (*CXCL9* and *IFNG*) of skin biopsies from a patient with (A) OS and (B) CID. Images are ×20 magnification, except for *IFNG* (×40). Scale bars, 50 µm. (**C**) Absolute eosinophil counts in the peripheral blood of patients with CID ($n = 31$), LS ($n = 19$), OS ($n = 39$), and SCID ($n = 23$). (**D**) IgE levels in the plasma of patients with CID ($n = 28$), LS ($n = 16$), OS ($n = 30$), and SCID ($n = 16$). The gray area in (C) and (D) indicates normal range in HDs. (**E**) $CD162^+CD4^+CD45RO^+$ cell frequency in HDs ($n = 53$) and patients with CID ($n = 31$), LS ($n = 20$), and OS ($n = 27$). (**F**) $CD162^+CD8^+CD45RO^+$ cell frequency in HDs ($n = 52$) and patients with CID ($n = 31$), LS ($n = 21$), and OS ($n = 26$). (**G**) $T_H$ cell subset distribution in HDs ($n = 64$) and patients with CID ($n = 29$), LS ($n = 19$), and OS ($n = 28$). (**H**) $T_{FH}$ cell subset distribution in HDs ($n = 62$) and patients with CID ($n = 29$), LS ($n = 18$), and OS ($n = 27$). (**I**) ILC subset distribution in HDs ($n = 29$) and patients with CID ($n = 28$), LS ($n = 18$), OS ($n = 22$), and SCID ($n = 9$). [(C) to (I)] Data from multiple independent experiments were pooled. Bars [(G) to (I)] show mean values ± SEM. Data were analyzed using [(C) to (F)] Kruskal-Wallis *H* test with Dunn's multiple comparisons test. [(G) to (I)] Asterisks reflect significant differences with HDs as a result of mixed-effects model with Geisser-Greenhouse correction and Benjamini, Krieger, and Yekutieli's multiple comparisons test. $*P < 0.05$, $**P < 0.005$, $***P < 0.001$, and $****P < 0.0001$.

biomarkers, such as interleukin-5 (IL-5), eosinophil-derived neurotoxin (EDN), CCL13, CCL17, CCL22, and CCL26. However, OS was also characterized by elevated plasma levels of molecules involved in type 1–associated responses [such as IL-12, interferon-γ (IFN-γ), CXCL9, and CXCL10] and type 3–associated responses (IL-17), as well as biomarkers indicative of monocyte activation [tumor necrosis factor–α (TNF-α), CCL2, and CCL3] (Fig. 4A). High levels of IFN-γ and IFN-γ–induced chemokines (CXCL9 and CXCL10) and other inflammatory mediators (CCL3, CCL4, CCL17, IL-8, IL-1α, IL-1β, and IL-6) were detected in all *RAG*-mutated patient groups (fig. S4), indicating that a dysregulated proinflammatory response is common to all forms of human RAG deficiency. By contrast,

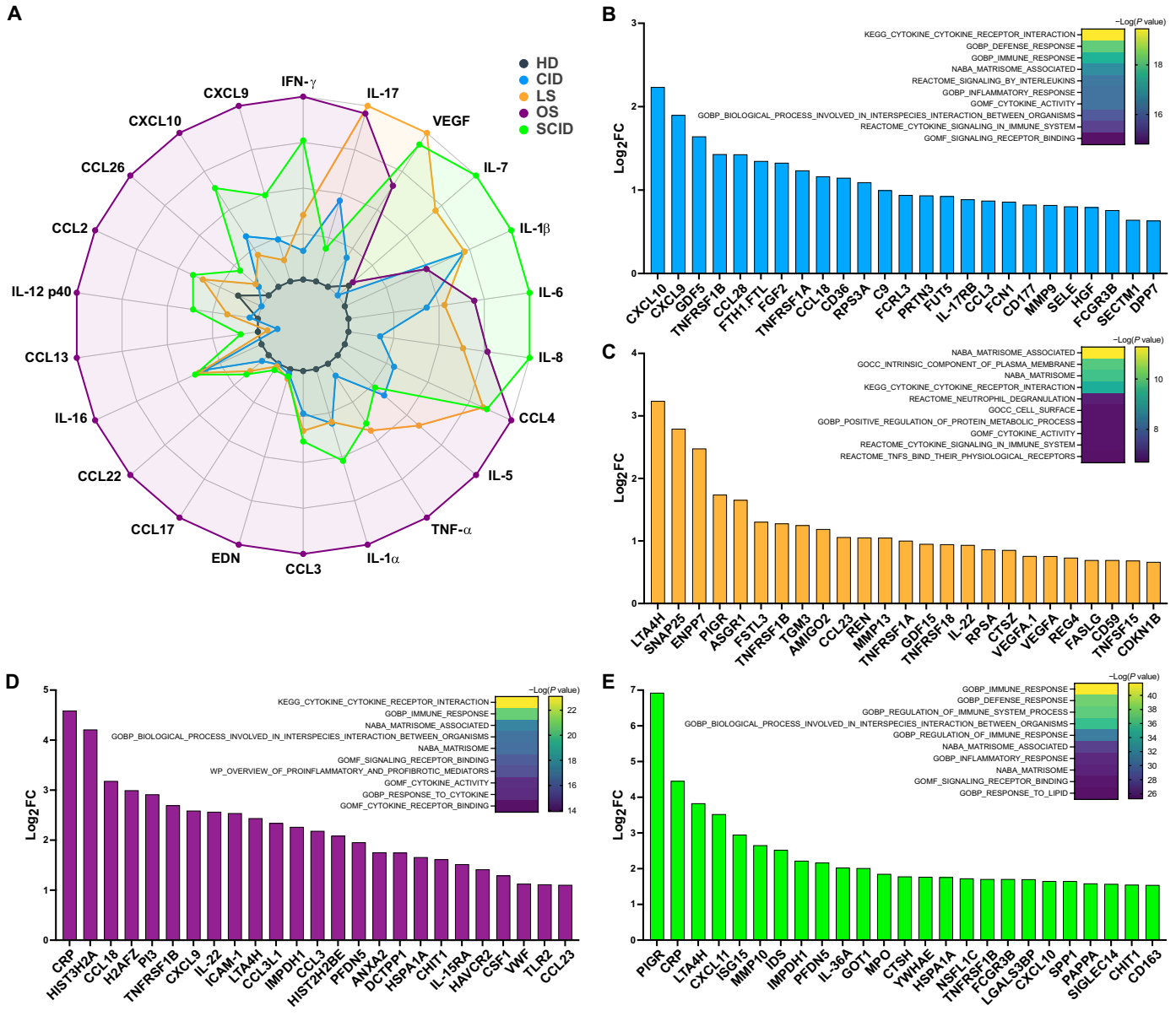


**Fig. 4. Broad inflammatory signature of *RAG*-mutated patients.** (**A**) Radar chart depicting 22 biomarkers in *RAG*-mutated patients and HDs. The graph shows the median value for each biomarker in each group. The radar chart is scaled to the maximum and minimum value for each biomarker. Data were pooled from multiple independent experiments. VEGF, vascular endothelial growth factor. (**B** to **E**) Proteomic analysis in *RAG*-mutated patients and HDs. Graphs show the top 25 plasma proteins up-regulated in each group of *RAG*-mutated patients ($n = 5$ individuals per group) versus HDs: (B) CID, (C) LS, (D) OS, and (E) SCID. Each group of patients was compared with an age-matched group of HDs ($n = 3$ to 6). Results for all groups were obtained in one experiment. Top up-regulated proteins were identified by selecting all proteins with FDR < 0.05 and $P < 0.05$ (two-tailed *t* test) and then ordering them according to increased fold changes expressed in a $\log_2$ scale ($\log_2$FC). Heatmaps inside each graph show the most significantly enriched pathways for the group comparison, and the statistical significance is expressed as −log(*P* value). FGF2, fibroblast growth factor 2; MMP9, matrix metalloproteinase 9; GDF15, growth and differentiation factor 15; CRP, complement-reactive protein; ICAM-1, intercellular adhesion molecule–1; CSF1, colony-stimulating factor 1; TLR2, Toll-like receptor 2; FTH1.FTL, ferritin heavy chain 1.ferritin light chain; RPS3A, ribosomal protein S3A; FCRL3, Fc receptor like 3; PRTN3, proteinase 3; FUT5, fucosyltransferase 5; FCN1, ficolin 1; SELE, E-selectin; HGF, hepatocyte growth factor; FCGR3B, Fc gamma receptor IIIb; SECTM1, secreted and transmembrane 1; DPP7, dipeptidylpeptidase 7; LTA4H, leukotriene A4 hydrolase; SNA25, synaptosome associated protein 25; ENPP7, ectonucleotide phosphatase/phosphodiesterase 3; PIGR, polymeric immunoglobulin receptor; ASGR1, asialoglycoprotein receptor 1; FSTL3, follistatin like 3; TGM3, transglutaminase 3; AMIGO2, adhesion molecule with Ig like domain 2; REN, renin; RPSA, ribosomal protein SA; CTSZ, cathepsin Z; REG4, regenerating family member 4; FASLG, Fas ligand; CDKN1B, cyclin dependent kinase inhibitor 1B; HIST3H2A, histone gene cluster 3 H2A; H2AFZ, histone 2A family member Z; PI3, peptidase inhibitor 3; IMPDH1, inosine monophosphate dehydrogenase 1; PFDN5, prefoldin subunit 5; ANXA2, annexin A2; DCTPP1, DCTP pyrophosphatase 1; HSPA1A, heat shock protein family A member 1A; CHIT1, chitinase 1; HAVCR2, hepatis A virus cellular receptor 2; VWF, von Willebrand factor; ISG15, interferon stimulated gene 15; IDS, iduronate 2-sulfatase; GOT1, glutamic-oxaloacetic transaminase 1; MPO, myeloperoxidase; CTSH, cathepsin H; YWHAE, tyrosine 3-monooxygenase/tryptophan 5-monooxygenase activation protein epsilon; NSFL1C, NSFL1 cofactor; FCGR3B, Fc gamma receptor IIIb; LGALS3BP, galectin 3 binding protein; SPP1, secreted phosphoprotein 1; PAPPA, pappalysin 1; SIGLEC14, sialic acid binding Ig like lectin 14.

high levels of IL-7, a cytokine essential for T cell development and survival, were detected only in the LS and SCID groups (Fig. 4A and fig. S4), likely reflecting their T cell lymphopenia.

We next used SomaScan to perform proteomic profiling in the plasma of 20 *RAG*-mutated patients and 12 controls. An IFN-γ signature (CXCL9, CXCL10, and CXCL11) was detected in patients with CID, OS, and SCID (Fig. 4, B to E). All patient groups had high levels of soluble TNF receptor 1 (TNFR1) (TNFRSF1A) and TNFR2 (TNFRSF1B) (Fig. 4, B to E). Furthermore, high levels of CCL3, CCL18, CCL23, and CD163 were also observed, indicative of macrophage activation. CCL18—a chemokine associated with atopic dermatitis (*18*)—was strongly enriched in the plasma of patients with OS (Fig. 4D). The polymeric immunoglobulin receptor (PIGR), whose expression is induced by proinflammatory cytokines (*19*), was particularly abundant in patients with LS and SCID (Fig. 4, C and E). Pathway analysis demonstrated signatures associated with cytokine–cytokine receptor interactions, immune responses, inflammatory responses, and matrisome activation in all groups of *RAG*-mutated patients (Fig. 4, B to E). Thus, an IFN-γ– and macrophage activation–dependent proinflammatory signature is present in all forms of RAG deficiency, whereas a type 2 immune response is specific to OS.

## A wide range of autoantibodies is detected in the plasma of *RAG*-mutated patients

We and others had previously demonstrated that the mature B cells of *RAG*-mutated patients with CID and LS are enriched for self-reactive specificities (*20*–*22*). To profile these specificities in greater detail, we subjected plasma from 10 *RAG*-mutated patients (4 CID, 3 LS, and 3 OS) and 10 HDs to the HuProt microarray. Patients with SCID were not included because they were agammaglobulinemic. *RAG*-mutated patients showed enhanced reactivity to a broad range of self-antigens (Fig. 5A and data file S9). A broad range of autoantibodies were also detected in patients with APECED (autoimmune polyendocrinopathy–candidiasis–ectodermal dystrophy) and those with thymoma, two conditions associated with abnormal development and function of thymic stromal cells (*23*, *24*). A strong reactivity against IFN-α peptides was observed in patients with CID and LS (as well as in patients with APECED and thymoma), but not in patients with OS (Fig. 5A). To confirm and expand on these results, we analyzed a larger group of *RAG*-mutated patients for the presence of autoantibodies against type I IFN (IFN-α, IFN-β, and IFN-ω) and of anti–IFN-λ antibodies (data file S10). High levels of anti–IFN-α antibodies were detected in most patients with CID and LS (31 of 39 and 17 of 29 patients, respectively), but not in those with OS and SCID (Fig. 5B). Furthermore, 28 of 39 patients with CID and 13 of 29 patients with LS had high levels of anti–IFN-ω antibodies (Fig. 5C). In most cases, these autoantibodies had neutralizing activity (data file S10). Increased levels of anti–IFN-β antibodies were detected in 18 of 39 patients with CID and in 10 of 29 patients with LS (Fig. 5D). Elevated levels of anti–IFN-λ antibodies were present in a minority of patients with CID (14 of 33) and in those with LS (6 of 22) (Fig. 5E). A low proportion of patients with CID and LS tested positive for other anticytokine antibodies targeting IL-12, IL-17A, IL-17F, IL-22, and IL-23 (fig. S5 and data file S10). Anticytokine antibodies were not detected in most patients with OS and SCID (Fig. 5, B to E, and fig. S5). Thus, *RAG*-mutated patients with LS and CID produce a broad range of autoantibodies, including neutralizing antibodies to type I IFN.

## The peripheral compartments of patients with CID and LS are enriched in dysfunctional B cells

To further investigate the immune dysregulation of patients with CID and LS, we analyzed their peripheral B cell compartment and observed that patients with CID and LS have a lower proportion of $IgD^+CD27^-$ naïve B cells and a slightly increased frequency of $IgD^-CD27^-$, unswitched memory ($IgD^+CD27^+$), and switched memory ($IgD^-CD27^+$) B cells compared with HDs (Fig. 6A and data file S11). Previous studies have shown a high frequency of $CD19^{hi}CD21^{lo}$ B cells in various conditions associated with prolonged B cell activation, including chronic infections and autoimmunity (*25*–*28*). These cells are enriched for B cell receptor (BCR) specificities for foreign antigens upon infection or immunization (*26*) or for self-antigens in the course of autoimmune diseases (*27*). The expansion of $CD19^{hi}CD21^{lo}$ B cells is promoted by an inflammatory milieu, particularly IFN-γ (*29*). Patients with CID and LS had an increased frequency of $CD19^{hi}CD21^{lo}$ B cells (Fig. 6, B to D), which correlated with both CXCL9 levels and the proportion of $T_{FH}1$ cells (Fig. 6, E and F). Among $CD19^{hi}CD21^{lo}$ B cells, a subset expressing T-bet and the myeloid marker CD11c has been identified, which, on the basis of the expression of IgD and CD27, can be further divided into multiple subtypes of atypical B cells, including $CD19^{hi}CD21^{lo}CD11c^+IgD^+CD27^-$ activated naïve B (aNaB), $CD19^{hi}CD21^{lo}CD11c^+IgD^-CD27^-$ double-negative 2 (DN2), and $CD19^{hi}CD21^{lo}CD11c^+CD27^+$ activated memory B (aMeB) cells (*30*) (fig. S6). Patients with CID and LS had a significantly higher proportion of aNaB, DN2, and aMeB cells than HDs (Fig. 6, G to I). Staining of circulating B cells with 9G4, a monoclonal anti-idiotype antibody recognizing polyreactive VH4-34–encoded antibodies (*31*–*34*), revealed that patients with CID and LS have a higher proportion of $9G4^+$ B cells compared with HDs (Fig. 6, J and K), including both $9G4^{hi}$ cells representing B cells expressing surface $VH4\text{-}34^+$ immunoglobulins (Fig. 6L) and $9G4^{int}$ cells representing B cells decorated by circulating VH4-34 antibodies (Fig. 6M) (*35*). The proportion of $9G4^+$ cells was enriched within $CD21^{lo}$ B cells compared with total $CD19^+$ cells, and, likewise, a higher proportion of $CD21^{lo}$ B cells was detected within $9G4^+$ than within total $CD19^+$ cells (Fig. 6, N and O). These data confirm and extend previous findings (*22*) that the peripheral B cell compartments of patients with hypomorphic forms of RAG deficiency are enriched in dysreactive B cells.

## Signatures of immune dysregulation in heterozygous carriers of *RAG* mutations and in patients with other forms of LS

The observation that heterozygous carriers have an intermediate proportion of $V\alpha7.2^+$ T cells between HDs and patients with biallelic *RAG* mutations prompted us to investigate these individuals for cellular and molecular signatures of immune dysregulation. CXCL9, CXCL10, IL-1β, and CCL4 plasma levels were increased in heterozygous individuals (fig. S7A and data file S8). In addition, a proportion of them had an increased percentage of $9G4^+$ and $9G4^{int}$ B cells (fig. S7B) and modestly elevated levels of anti–type I IFN antibodies, which, however, were nonneutralizing (fig. S7C and data file S10). Thus, individuals with heterozygous *RAG* mutations may present subtle biological signatures of immune dysregulation, although they do not manifest clinically overt autoimmune disease.

To investigate whether these signatures of immune dysregulation are unique to hypomorphic RAG deficiency, we analyzed samples from 16 patients with other defects of adaptive immunity. Higher levels of soluble inflammatory biomarkers and of anti–type I IFN

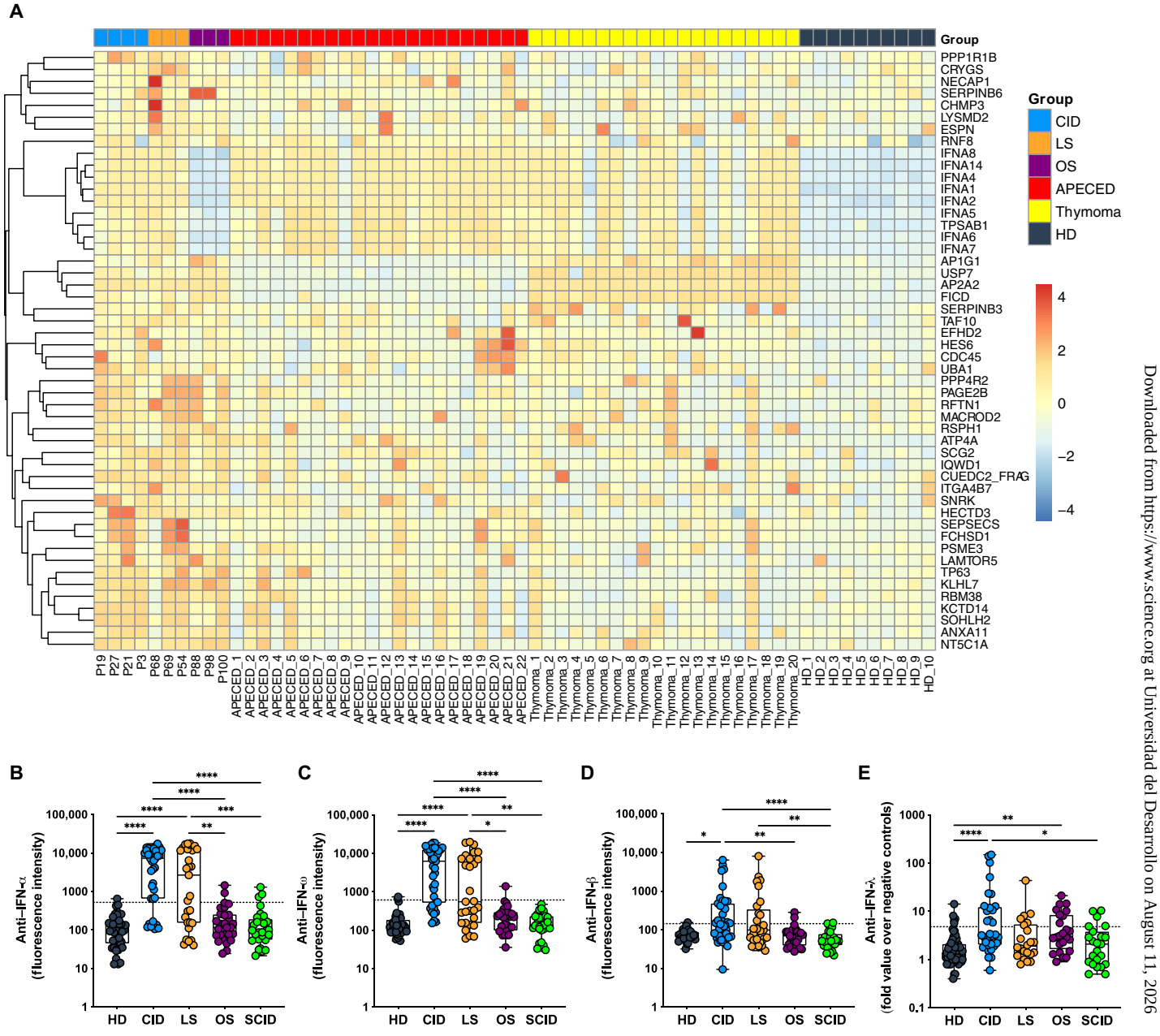


**Fig. 5. Characterization of the autoantibody profile in the plasma of *RAG*-mutated patients.** (**A**) Heatmap showing the top 50 peptides to which autoantibody reactivity was detected in plasma from *RAG*-mutated patients using the HuProt assay. Each column represents a patient sample: CID, $n = 4$; LS, $n = 3$; OS, $n = 3$; APECED, $n = 22$; thymoma, $n = 20$; HD, $n = 10$. Results for all groups were obtained in one experiment. PPP1R1B, protein phosphatase 1 regulatory inhibitory subunit 1B; CRYGS, crystallin gamma S; NECAP1, NECAP endocytosis associated protein 1; SERPINB6, serpin family B member 6; CHMP3, charged multivesicular body protein 3; LYSMD2, LysM domain containing protein 2; ESPN, espin; RNF8, ring finger protein 8; IFNA8, interferon alpha 8; TPSAB1, tryptase alpha/beta 1; APIG1, adaptor related protein complex 1 subunit gamma 1; USP7, ubiquitin specific peptidase 7; AP2A2, adaptor protein complex 2 subunit alpha 2; FICD, FIC domain containing protein; SERPINB3, serpin family B member 3; TAF10, TATA-box binding protein associated factor 10; EFHD2, EF-Hand domain family member D2; HES6, HES family BHLH transcription factor 6; CDC45, cell division cycle 45; UBA1, ubiquitin like modifier activating enzyme 1; PPP4R2, protein phosphatase 4 regulatory protein 2; PAGE2B, PAGE family member 2B; RFTN1, raftin lipid raft linker 1; MACROD2, mono-ADP ribosylhydrolase 2; RSPH1, radial spoke head component 1; ATP4A, ATPase H+/K+ transporting subunit alpha; SCG2, secretogranin 2; IQWD1, IQ motif and WD repeat-containing protein 1; CUEDC2_FRAG, CUE domain containing 2; ITGA4B7, integrin subunit alpha 4 beta 7; SNRK, SNF related kinase; HECTD3, HECT domain 3 ubiquitin protein ligase 3; SEPSECS, SEP (O-phosphoserine) TRNA:Sec (selenocysteine) TRNA synthase; FCHSD1, FCH and double SH3 domains 1; PSME3, proteasome activator subunit 3; LAMTOR5, late endosomal/lysosomal adaptor MAPK and MTOR activator 5; TP63, tumor protein P63; KLHL7, Kelch like family member 7; RBM38, RNA binding motif protein 38; KCTD14, potassium channel tetramerization domain containing 14; SOHLH2, spermatogenesis and oogenesis specific basic helix-loop-helix 2; ANXA11, annexin A 11; NT5C1A, 5′-nucleotidase cytosolic IA. (**B** to **E**) Box-and-whisker plots with scatter dot plots showing the fluorescence intensity of (B) anti–IFN-α, (C) anti–IFN-ω, and (D) anti–IFN-β antibodies detected in the plasma of HDs ($n = 43$) and patients with CID ($n = 38$), LS ($n = 29$), OS ($n = 30$), and SCID ($n = 29$). (E) Box-and-whisker plots with scatter dot plots showing the quantification of anti–IFN-λ antibodies as reactive luciferase units in the plasma of HDs ($n = 67$) and patients with CID ($n = 33$), LS ($n = 22$), OS ($n = 24$), and SCID ($n = 23$). [(B) to (E)] Data from multiple independent experiments were pooled. The dashed lines in (B) to (E) represent the upper limit of normal defined as means + 3 SD in HDs. Asterisks in (B) to (E) reflect *P* values results of Kruskal-Wallis *H* test, followed by Dunn's multiple comparisons test. $*P < 0.05$, $**P < 0.005$, $***P < 0.001$, and $****P < 0.0001$.

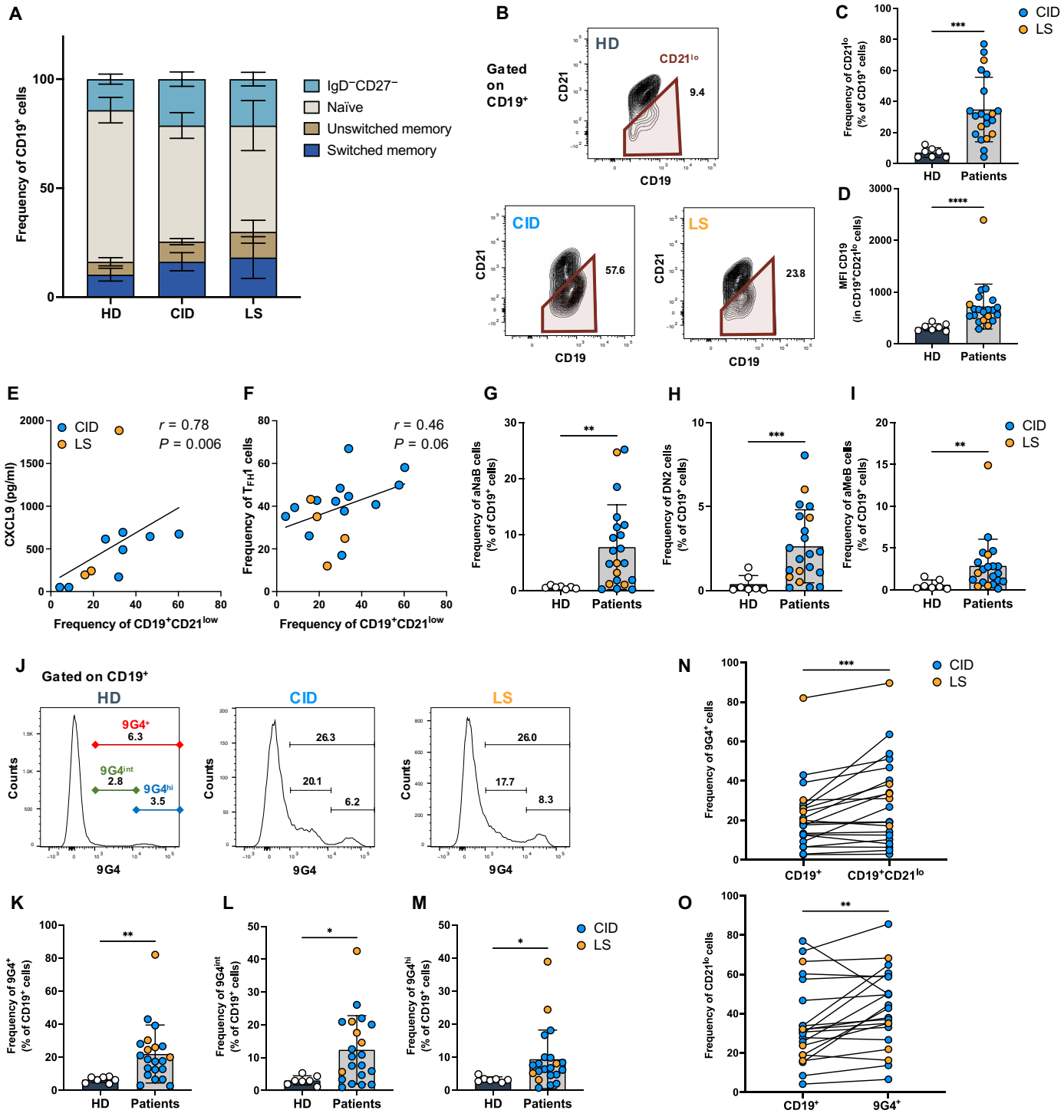


**Fig. 6. Analysis of B cell subset distribution and dysreactive B cells in peripheral blood of *RAG*-mutated patients.** (**A**) Stacked bar graph showing the distribution of naïve and memory B cell subsets in the peripheral blood of HDs ($n = 7$) and patients with CID ($n = 16$) and LS ($n = 5$). Bars show mean values ± SEM. (**B**) Representative plots showing the frequency of $CD19^+CD21^{lo}$ cells gated on total $CD19^+$ cells. (**C** and **D**) Bar graphs with scatter dot plots summarizing the frequency of the $CD21^{lo}$ in total B cells (C) and the mean fluorescence intensity (MFI) of CD19 in $CD19^+CD21^{lo}$ cells (D). (**E** and **F**) Graphs show the correlation between the frequency of $CD21^{lo}$ B cells and the concentration of (E) CXCL9 or (F) the frequency of $T_{FH}1$ cells. Linear regression curve is shown in each graph along with the Spearman correlation factor ($r$) and $P$ value. (**G** to **I**) Bar graphs showing the frequency of atypical B cells: (G) aNaB, (H) DN2, and (I) aMeB cells. (**J**) Representative plots showing the frequency of 9G4-positive cells ($9G4^+$, $9G4^{hi}$, and $9G4^{int}$) gated on total $CD19^+$ cells. (**K** to **M**) Bar graphs showing the frequency of (K) $9G4^+$, (L) $9G4^{int}$, and (M) $9G4^{hi}$ cells gated on total $CD19^+$ B cells. (**N** and **O**) Graphs showing (N) the frequency of $9G4^+$ cells among $CD19^+$ and $CD19^+CD21^{lo}$ cells and (O) the frequency of $CD21^{lo}$ cells among $CD19^+$ and $9G4^+$ cells in patients with CID and LS. The lines connect the values found in the same individual. [(A) to (D) and (G) to (O)] Data were pooled from two independent experiments. [(C), (D), (G) to (I), and (K) to (M)] Bars represent means ± SD. (A) Mixed-effects model with Geisser-Greenhouse correction and Benjamini, Krieger, and Yekutieli's multiple comparisons test. [(C), (D), (G) to (I), and (K) to (M)] Mann-Whitney $U$ test, two-tailed. [(N) and (O)] Spearman correlation test. *$P < 0.05$, **$P < 0.005$, ***$P < 0.001$, and ****$P < 0.0001$.

antibodies were detected in several of them, especially in those with hypomorphic *DCLRE1C* and CD3 chain defects (fig. S7, A and C, and data file S8). Furthermore, immunohistochemistry and RNAscope analysis of a skin biopsy from a patient with hypomorphic DNA cross-link repair 1C (DCLRE1C) deficiency revealed a strong IFN-γ/CXCL9 signature (fig. S7D). Thus, the inflammatory signatures observed in *RAG*-mutated patients are not only found in this condition but can also be observed in other genetic defects affecting adaptive immunity.

### Single-cell profiling reveals phenotype-specific signatures of inflammation and immune dysregulation in *RAG*-mutated patients

To further investigate the immune cell type–specific signatures of inflammation and immune dysregulation, we performed single-cell cellular indexing of transcriptomes and epitopes by sequencing (CITE-seq) in peripheral blood mononuclear cells (PBMCs) from 11 *RAG*-mutated patients (3 CID, 3 OS, 3 SCID, and 2 LS) and seven HDs, revealing five major subsets of immune cells: CD4 T cells, CD8 T cells, NK cells, B cells, and myeloid cells [comprising monocytes and dendritic cells (DCs)] (Fig. 7A). A low frequency of CD4 T cells that were represented almost exclusively by memory cells was detected in *RAG*-mutated patients, with a small fraction of naïve CD4 T cells and regulatory T cells ($T_{regs}$) present only in patients with CID and LS (Fig. 7, B and C). CD8 T cells were present with reduced frequency in patients with CID and LS and nearly absent in patients with SCID but were increased in the OS group. However, in all groups of *RAG*-mutated patients, CD8 T cells were mostly memory cells. $CD16^+$ cells represented most NK cells in all groups of *RAG*-mutated patients and controls. Circulating B cells were nearly absent in the SCID and OS groups and represented a lower fraction of PBMCs in patients with CID but were present at higher frequency in patients with LS, where they were predominantly represented by B intermediate cells (*36*). Last, classical $CD14^+$ monocytes represented a high fraction of PBMCs in patients with SCID, consistent with the severe lymphopenia of this condition.

Hallmark pathway analysis revealed a prominent inflammatory signature, dominated by TNF-α, IFN-γ, and IFN-α response in multiple PBMC types from all groups of *RAG*-mutated patients compared with HDs (Fig. 7, D and E). Signatures of immune activation in *RAG*-mutated patients included enrichment for IL-6–Janus kinase (JAK)–signal transducers and activators of transcription 3 (STAT3), IL-2–JAK–STAT5, and mammalian target of rapamycin (mTOR) signaling pathways (Fig. 7D). Apoptosis and hypoxia pathways were also up-regulated in PBMCs from *RAG*-mutated patients (Fig. 7D). Analysis of gene expression profiles of circulating T cells demonstrated enhanced expression of *TBX21* in patients with CID and of *GATA3* in patients with OS (Fig. 7F), confirming the differences in type 1–type 2 phenotype of these conditions.

To better define the contribution of individual PBMC subsets to these signatures, we performed RNA-based subclustering within all major PBMC subsets and identified the relative representation of each subcluster in HDs and in each group of *RAG*-mutated patients (fig. S8 to S12, A to D). The CID group was characterized by CD4 cells with increased surface expression of CD2 and CD48 (fig. S8E) and enhanced expression of *JUN* and *ZFP36*—an RNA binding protein that regulates the stability of *IFNG* and other mRNAs involved in inflammatory responses (fig. S8F) (*37*). Hallmark pathway analysis revealed TNF-α signaling and hypoxia as signatures of CD4 cells (fig. S8G). CD8 cells from patients with CID showed a prominent IFN-α and IFN-γ signature, driven by higher expression levels of *OASL*, *IFIT3*, and *IFIT2* and increased surface levels of CD2 and CD48 (fig. S9, E to G). NK cells had prominent IFN-α and TNF-α signatures, with enhanced expression of *IFIT1*, *ISG20*, *OASL*, *HERC5*, and *IFIH1* (fig. S10, E to G). CID myeloid cells were predominantly represented by $CD33^+CD35^+$ classical monocytes expressing higher levels of *MAP3K8*, which promotes hypoxia-induced release of TNF-α (*38*), and were characterized by an IL-6–JAK–STAT3 and TNF-α signaling signature (fig. S11, E to G). Thus, multiple immune cell subsets contribute to the type 1 immunopathology observed in the CID group.

A similar proinflammatory signature was observed in multiple PBMC subsets from patients with LS. In particular, their CD4 cells expressed higher levels of *MT2A*, a metallothionein family member with a scavenger function for reactive oxygen species (ROS) (*39*), and *IRF1*, a transcription factor that plays a critical role in $T_H1$ differentiation (*40*) (fig. S8F). Pathway analysis identified IFN-α and IFN-γ response, IL-6–JAK–STAT3 signaling, ROS, oxidative phosphorylation (OXPHOS), and fatty acid metabolism as signatures of LS CD4 cells (fig. S8G). CD8 T cells had prominent TNF-α, IFN-α, and IFN-γ signaling signatures (fig. S9F). A TNF-α signature was also present in NK cells (fig. S10, D and G). Last, myeloid cells from patients with LS had higher levels of *ID1*, *IL1B*, and *CCL3* expression (fig. S11F) and OXPHOS, ROS, and fatty acid metabolism signatures (fig. S11G).

The predominant type 2 immunopathology profile of OS was supported by CD4 cells with higher expression levels of CCR4 protein (fig. S8H), as well as of *LGALS1* and *S100A4* transcripts (fig. S8F). *LGALS1* encodes for galectin-1, whose immunomodulatory properties skew immune response toward a type 2 profile (*41*). S100A4 is an alarmin preferentially expressed by effector memory T cells that participate in allergic inflammation (*42*). Pathway analysis showed that OS CD4 T cells had a signature characterized by enhanced unfolded protein response, hypoxia, TNF-α and mTOR signaling, ROS and OXPHOS, cholesterol homeostasis, and apoptosis (fig. S8G). CD8 T cells from patients with OS expressed higher surface levels of CD99, which is associated with the recruitment of T cells into inflamed skin (*43*) (fig. S9E), and had strong TNF-α and mTOR signaling signatures (fig. S9G). OS myeloid cells had increased levels of *SERPINB2* and *SERTAD1* (fig. S11F), which modulate type 1 versus type 2 immune responses (*44*) and initiate NLR family porin domain-containing protein 3 (NLRP3)–mediated inflammasome activation (*45*), respectively. TNF-α signaling and OXPHOS were signatures of OS myeloid cells. A similar inflammatory signature (driven by TNF-α, IFN-α, and IFN-γ) was present in monocytes from patients with SCID (fig. S11G).

To better define the molecular and cellular basis of autoimmunity in patients with CID and LS, we analyzed the transcriptional and surface protein profile of circulating B cells. Most B cells from patients with CID were included in subcluster 10, characterized by higher levels of CD27 and CXCR3 expression (fig. S12E), suggesting that they represent memory B cells poised to migrate to inflamed tissues. The B cell compartments of patients with LS were more heterogeneous (fig. S12, C and D) and included a subset of cells (subcluster 9) with high levels of CD19 and CD11c, low levels of CD21 and IgD, and increased expression of *CD80*, *CD86*, and *ITGAX* (encoding for CD11c) transcripts (fig. S12E), indicative of an atypical B cell profile. Flow cytometry confirmed that B cells from patients with CID and LS were enriched in $CD21^{lo}CXCR3^+$ cells and in $CD21^{lo}CD11c^+$ atypical B cells (fig. S12, F and G). In addition, cells

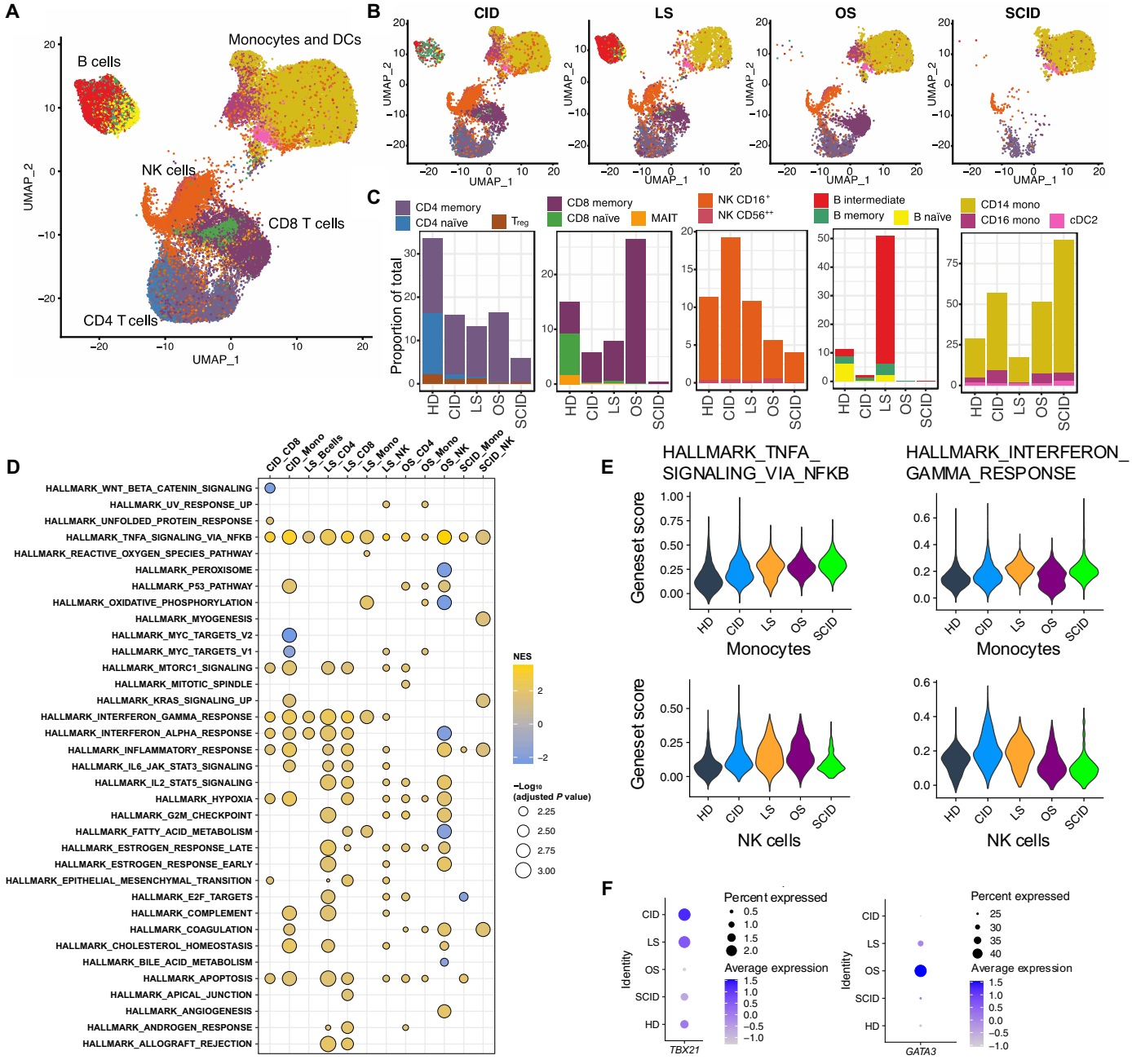


**Fig. 7. Single-cell CITE-seq profiling of peripheral blood cells of *RAG*-mutated patients.** (**A**) Uniform Manifold Approximation and Projection (UMAP) visualization of single-cell clusters based on surface protein expression profiles, obtained from PBMCs of HDs and patients combined. (**B**) Visualization of cells from each of the patient groups projected onto the same UMAP. (**C**) Distribution of the different CD4 T cell, CD8 T cell, NK cell, B cell, and monocyte subclusters in HDs and in each of the patient groups. (**D**) Cell type–specific GSEA map obtained by comparing each group of patients versus the HDs for the indicated cell type. Hallmark gene sets/pathways significantly enriched in *RAG*-mutated patients as compared with HDs are represented in each row, whereas each column indicates the cell type and patient group for which a difference versus HDs has been observed. Dot color denotes normalized gene set enrichment score, and size indicates $-\log_{10}$(adjusted *P* value). *P* values were computed from GSEA test of the whole gene sets and adjusted using the Benjamini-Hochberg method. NES, normalized enrichment score. (**E**) Violin plots showing the single-cell distribution of gene set score of selected Hallmark pathways (TNF-α signaling via NF-κB on the left and IFN-γ response on the right) in HDs and in each group of *RAG*-mutated patients in monocytes (top row) and NK cells (bottom row). (**F**) Average expression and percentage of cells expressing the transcription factors (*TBX21* and *GATA3*) among CD4 T memory cells in each of the patient groups and in HDs. Results were from a single experiment in all groups of patients and controls.

in subclusters 0, 1, and 3 from patients with LS shared higher levels of *CD19* and *TBX21* transcripts and low levels of CD21 protein (fig. S12E) and may also represent atypical B cells. Pathway analysis demonstrated that subclusters of B cells overrepresented in LS have OXPHOS, ROS, IFN-α, and fatty acid metabolism signatures (fig. S12H).

V(D)J sequencing analysis demonstrated that all VH4-34$^{+}$ B cell clonotypes detected in patients with CID were accounted for by B

cells in subcluster 10 (table S1), whereas the VH4-34$^+$ B cell clonotypes of patients with LS were distributed across various B cell clusters, with most of them (24 of 44, 54.5%) belonging to subcluster 6, characterized by an inflammatory signature (IFN-α, IFN-γ, TNF-α, and IL-6–JAK–STAT3 signaling). Overall, the frequencies of VH4-34 B cell clonotypes were not increased in patients with LS and CID (1.3 and 5.3% of all unique B cell clonotypes, respectively) compared with HDs (6.0%) (table S1). Somatic hypermutation at the AVY amino acid residues in the framework region 1 (FR1) and the *N*-hydroxysuccinimide residues in the complementarity-determining region 2 (CDR2) has been shown to redeem VH4-34 antibodies, depriving them of self-reactivity (*34*). Missense variants at these positions were detected at a similar frequency in VH4-34 clonotypes from patients with CID (1 of 11, 9.1%) and LS (6 of 44, 13.6%), as compared to HDs (12 of 92, 13.0%) (table S1). Thus, an increased frequency of atypical B cells with a proinflammatory phenotype may contribute to the immune dysregulation seen in patients with CID and LS.

## DISCUSSION

We used a multiomics approach to characterizing the molecular and immunological features of human RAG deficiency, identifying both common and distinctive signatures associated with its clinical phenotypes. By analyzing numerous naturally occurring *RAG* variants, we expanded on the genotype-phenotype correlation, confirming that CID and LS phenotypes are associated with residual functional activity of the mutant alleles (*11*, *12*). We have also confirmed that human *RAG* variants allow DP T cell development in vitro, regardless of variant severity (*14*). This developmental block contrasts with the earlier block at the CD44$^-$CD25$^+$ DN3 stage reported in *Rag1*$^{-/-}$ and *Rag2*$^{-/-}$ mice (*46*, *47*). In the bone marrow of *RAG*-mutated patients, we observed a block at the pro-B/pre-B I stage. However, this block was incomplete in patients with LS and CID, allowing the generation of a residual number of immature and mature B cells. These observations have important implications because they suggest that competition between autologous and allogeneic donor cells may occur until the DP stage of T cell development and the pre-B I stage of B cell development after unconditioned HSCT, leading to incomplete immune reconstitution (*48*, *49*).

By studying the proportion of T cells stained by the Vα7.2 monoclonal antibody, we confirmed that human RAG deficiency is associated with a skewed pattern of rearrangements at the *TRA* locus, with reduced usage of 5′ *TRAV* and 3′ *TRAJ* genes (*15*). This pattern was observed irrespective of disease severity. We also found that individuals heterozygous for loss-of-function *RAG* variants had proportions of Vα7.2$^+$ T cells intermediate between those of HDs and *RAG*-mutated patients. Previous studies have shown higher levels of *RAG* expression in DP T cells (*50*) due to retinoid acid receptor–related orphan receptor γt (RORγt) binding to a DP-specific component of the recombination activating genes antisilencer enhancer, driving *RAG* expression at the DP stage and facilitating secondary rearrangements involving 5′ *TRAV* and 3′ *TRAJ* genes (*51*). Consistent with those reports and mirroring our present findings in individuals heterozygous for deleterious *RAG* variants, *Rag1*$^{+/-}$ mice show reduced usage of these genes (*51*).

Prominent signatures of immune dysregulation, with common and distinctive features, were identified in all groups of *RAG*-mutated patients. In particular, a strong systemic and cutaneous type 2 signature was detected in patients with OS. Previous studies have shown that PBMCs from patients with OS produce high levels of IL-4 and IL-5 in vitro (*52*), consistent with the hyper-IgE phenotype and eosinophilia of OS. In addition, studies in hypomorphic *Rag1*-mutant mice have shown that perturbed B cell development may also contribute to the hyper-IgE phenotype through direct class switching from Cμ to Cε in CD93$^+$ B cell progenitors (*53*). Here, we demonstrated that OS is characterized by an increased frequency of circulating memory T cells with a $T_H2$ phenotype, high plasma levels of CCL17 and CCL22 (ligands for the $T_H2$ chemokine receptor CCR4) (*54*), as well as CCL13 and CCL26, implicated in cutaneous allergic disease (*55*, *56*). RNAscope analysis of skin biopsies and CITE-seq analysis of PBMCs from patients with OS demonstrated increased proportions of T cells expressing *GATA3*, the prototypic transcription factor involved in $T_H2$ cell differentiation.

Our CITE-seq data demonstrated that circulating CD4 and CD8 T cells from patients with OS express higher levels of CD99, a glycoprotein involved in recruiting T cells into inflamed skin (*43*). Together, these data establish OS as a condition with an increased frequency of $T_H2$ cells poised to migrate to the skin, driving tissue immunopathology. In addition, the increased frequency of ILC2s suggests that other cell types may contribute to the immune dysregulation and enhanced production of IL-4, IL-5, and IL-13, characterizing OS as dominated by a type 2 signature. Unexpectedly, a strong IFN-γ signature was observed in the skin biopsies and peripheral blood of patients with OS. High levels of IFN-γ, CXCL9, and CXCL10 had been reported in patients with OS and in a mouse model (*Rag2*$^{R229Q/R229Q}$) of this disease (*57*, *58*). It has been suggested that the immunodeficiency of this condition may favor microbiome abnormalities and breaches in the cutaneous and gastrointestinal barriers, leading to bacterial translocation and promoting systemic inflammation and accumulation of pathological $T_H1$ and $T_H17$ cells in the intestinal lamina propria (*57*, *58*). Broad immunosuppressive agents (e.g., steroids, cyclosporine A, and tacrolimus) are often needed to control the inflammatory phenotype of OS. Dupilumab, a monoclonal antibody targeting the IL-4Rα chain, has been used to treat severe atopic dermatitis (*59*). However, the in vitro addition of dupilumab to CD4 T cells from a patient with OS had only modest effects on IL-4 production, suggesting that activated T cells from patients with OS may not depend solely on IL-4 signaling for the production of type 2 cytokines (*60*). In vivo treatment with IFN-γ has been proposed to revert the type 2 phenotype of OS. Although eosinophil count improved, elevated IgE levels and increased proportion of activated/memory CD4 T cells persisted (*52*), suggesting that pharmacological agents with a broad effect on T cells and macrophages are needed to control the hyperinflammatory signature of OS.

A strong type 1 inflammatory signature was also detected in the granulomatous lesions and plasma of patients with CID, as demonstrated by the expression of *TBX21* and by the IFN-γ signature associated with skin granulomas. Persistence of the rubella virus vaccine strain has been documented in several patients with RAG-associated CID (*61*, *62*), including some in this study, and may play a role in the development of granulomatous lesions and chronic inflammation.

The inflammatory signatures of RAG deficiency may be secondary to recurrent and/or persistent infections, as suggested by similar observations in patients with other defects of adaptive immunity. Limited and mostly transient success has been reported with use of biologicals (e.g., emapalumab, infliximab, adalimumab, and ustekinumab), or of small molecules, such as JAK inhibitors as anti-inflammatory agents in

RAG deficiency (*63*). This approach could help prevent organ damage, which has a negative impact on the outcome of HSCT (*10*), but the potential benefits must be weighed against the increased risk of infections.

In addition to inflammation, autoimmunity is another prominent feature of immune dysregulation in patients carrying hypomorphic *RAG* variants. Analysis of these patients' peripheral B cell compartments demonstrated an increased proportion of CD19$^{hi}$CD21$^{lo}$ B cells, many of which coexpressed CD11c and CXCR3, suggesting their propensity to migrate to inflammatory sites. It has been shown that in vitro stimulation of HD B cells with anti-IgM and IFN-γ can induce CD21$^{lo}$ B cells (*29*). We observed a strong correlation between the proportions of CD21$^{lo}$ B cells detected in patients with CID and LS and CXCL9 levels and percentages of $T_{FH}1$ cells. The inflammatory milieu and elevated B cell activating factor (BAFF) levels observed in *RAG*-mutated patients with CID and LS may promote the activation of atypical B cells and their differentiation into autoantibody-producing plasma cells. The HuProt autoantibody array revealed a broad spectrum of autoantibody specificities in patients with CID and LS, similar to results reported using phage immunoprecipitation sequencing (*64*). Autoimmune cytopenias are a frequent complication of CID and LS and are often refractory not only to steroids but also to rituximab (*63*), suggesting that plasma cell–depleting agents (bortezomib and daratumumab) may be beneficial.

In this study, we observed that 9G4 monoclonal antibody marked a high proportion of circulating B cells from patients with CID and LS. However, CITE-seq analysis failed to reveal an increased proportion of B cells expressing *VH4-34* immunoglobulin transcripts. Similar observations have been recently reported (*22*). It has been demonstrated that circulating VH4-34 antibodies can also bind to a CD45 glycoform expressed on the surface of B cells (*35*). Higher plasma levels of VH4-34 antibodies may account for the decoration of circulating B cells from patients with CID and LS observed in this study.

Among 68 patients with CID and LS for whom we had clinical data available, 50 tested positive for anti–IFN-α and/or anti–IFN-ω antibodies. Anti–type I IFN antibodies are a hallmark of APECED, a condition due to *AIRE* mutations affecting expression of tissue-restricted antigens (TRAs) in the thymus, resulting in impaired negative selection of self-reactive T cells (*65*). Defects affecting the noncanonical nuclear factor κB (NF-κB) signaling pathway compromise *AIRE* expression and allow production of anti–type I IFN antibodies (*66*). Receptor activator of NF-κB (RANK) and CD40 signals provided by CD4$^+$ thymocytes promote noncanonical NF-κB pathway activation in medullary thymic epithelial cells (*67*). The reduced generation of CD4$^+$ thymocytes in *RAG*-mutated patients may be responsible for the impaired expression of *AIRE* and TRAs and the abnormalities of the $T_{reg}$ TCR repertoire that have been demonstrated under this condition (*68*–*70*). Neutralizing anti–type I IFN antibodies represent a risk factor for life-threatening viral infections (*71*–*74*). Among 50 *RAG*-mutated patients with anti–type I IFN antibodies included in his study, 31 had a history of severe or chronic viral infections. Epstein-Barr virus and cytomegalovirus viremia were recorded in 10 and 7 of these patients, respectively. Severe varicella (including vaccine-induced varicella) was observed in six patients, and severe herpes simplex virus, severe acute respiratory syndrome coronavirus 2, and human papillomavirus infections were detected in five patients each.

This study has some limitations. Some assays were performed in a subcohort of patients because of availability of samples and costs. Moreover, each patient was evaluated at a single time, so no longitudinal assessment of immune status was possible. Last, immunomodulatory treatments may also have affected results. Nonetheless, we were able to characterize the systemic and tissue-specific inflammatory and immune dysregulation signatures of human RAG deficiency. This study exemplifies the diversity of immune abnormalities associated with mutations of different degrees of severity in the same gene. These results may help design phenotype-specific pharmacological interventions while preparing for definitive therapy.

## MATERIALS AND METHODS

### Study design

We aimed to examine the immunological and molecular correlates of phenotypic heterogeneity of human RAG deficiency, using a multiomics approach.

### Patients

The study included 157 patients with biallelic *RAG* mutations encompassing the entire phenotypic spectrum of the disease: CID ($n = 46$), LS ($n = 33$), OS ($n = 44$), and SCID ($n = 34$), 40 apparently healthy individuals carrying heterozygous deleterious *RAG* variants, 16 patients with SCID/LS/CID due to other gene defects (*IL2RG*, $n = 6$; *IL7R*, $n = 1$; *DCLRE1C*, $n = 1$; *LIG4*, $n = 2$; *CD3E*, $n = 2$; *CD3G*, $n = 2$, *CORO1A*, $n = 1$; *TPP2*, $n = 1$) (data file S2) and 135 age-matched HDs. PBMC and bone marrow samples were obtained upon written informed consent, according to protocols NCT03394053 and NCT03610802 approved by the National Institutes of Health Institutional Review Board.

### Recombination activity of the mutant RAG alleles

Recombination activity of the mutant *RAG1* and *RAG2* alleles was tested using a flow cytometry–based reporter assay as described (*11*, *12*). Statistical analysis was performed by Kruskal-Wallis test for multiple comparisons, including for each patient the recombination activity of each mutant allele.

### Immune phenotyping, in vitro T cell differentiation, soluble biomarkers, proteomics, autoantibodies, and anticytokine antibodies

Peripheral blood samples were processed using Ficoll (GE Healthcare, Marlborough, MA). Single-cell suspensions were stained with monoclonal antibodies directed against cell surface molecules and analyzed by flow cytometry (table S3). $T_H$ cells were obtained after gating on CD4$^+$CD45RA$^-$CD25$^-$CXCR5$^-$ cells, and the different subsets were identified using the following markers: $T_H1$ (CXCR3$^+$CCR6$^-$CCR4$^-$), $T_H1$* (CXCR3$^+$CCR6$^+$CCR4$^-$), $T_H17$ (CXCR3$^-$CCR6$^+$CCR4$^-$), and $T_H2$ (CXCR3$^-$CCR6$^-$CCR4$^+$) cells. $T_{FH}$ cells were obtained after gating on CD4$^+$CD45RA$^-$CD25$^-$CXCR5$^+$ cells. Various $T_{FH}$ cell subsets were then identified using the following markers: $T_{FH}1$ (CXCR3$^+$CCR6$^-$CCR4$^-$), $T_{FH}17$ (CXCR3$^-$CCR6$^+$CCR4$^-$), and $T_{FH}2$ (CXCR3$^-$CCR6$^-$CCR4$^+$) cells. ILCs were obtained after gating on CD45$^+$Lin$^-$CD127$^+$ cells. Various ILC subsets were then identified using the following markers: ILC1s (CD117$^-$CD294$^-$), ILC2s (CD117$^-$CD294$^+$), and ILC3s (CD117$^+$CD294$^-$).

B cell maturation in bone marrow aspirates was assessed by flow cytometry using a panel of monoclonal antibodies directed against cell

surface markers. Pro-B cells were defined as $CD45^+CD34^+CD19^-CD22^+$ cells, pre-B I cells as $CD45^+CD34^+CD19^+$, large pre-B II cells as $CD45^+CD34^-CD19^+CD10^+CD20^-$, small pre-B II cells as $CD45^+CD34^-CD19^+CD10^+CD20^{lo}$, immature B cells as $CD45^+CD34^-CD19^+CD10^+CD20^+$, mature/recirculating B cells as $CD45^+CD34^-CD19^+CD10^-CD20^+$, and plasma cells as $CD45^+CD34^-CD19^+CD38^{hi}CD138^+$.

In vitro T cell differentiation studies were performed in 13 *RAG*-mutated patients (8 CID, 1 LS, 3 OS, and 1 SCID) and 11 HDs by coculturing peripheral blood or bone marrow $CD34^+$ cells in the ATO system and monitoring the progression of T cell differentiation over time by flow cytometry as previously described (*14*). Soluble biomarker plasma levels were analyzed in 127 *RAG*-mutated patients (38 CID, 31 LS, 32 OS, 26 SCID) and in 82 HDs using the V-PLEX Human Cytokine 30-Plex Kit (Meso Scale Discovery) and analyzed on a MESO QuickPlex SQ 120 reader (Meso Scale Discovery) or using a customized, magnetic bead–based, multiplex assay (R&D Systems), depending on the nature of analyte, as previously described (*75*). CXCL9 plasma levels were determined by enzyme-linked immunosorbent assay as described (*76*).

SomaScan (SomaLogic) was used to measure 1305 human protein analytes in plasma from 20 *RAG*-mutated patients (5 each for the CID, LS, OS, and SCID groups) and 12 HDs, as previously described (*75*). Statistical analysis was performed using R Studio (R Core Team, 2020). For each group comparison, top up-regulated and down-regulated proteins were identified by selecting all the proteins with false discovery rate (FDR) $< 0.05$ and $P < 0.05$. Pathway enrichment analysis was performed on differentially expressed biomarkers among the groups (CID, LS, OS, SCID, and HDs), using the Molecular Signatures Database version 7.4, as previously described (*75*).

IgG autoantibody analysis was performed on plasma samples from 10 *RAG*-mutated patients (4 CID, 3 LS, and 3 OS), 22 patients with APECED, 20 patients with thymoma, and 10 HDs using the HuProt version 4.0 human protein microarrays and processed by CDI Laboratories, as previously described (*75*). The quantile-normalized HuProt data were $\log_2$ transformed and filtered to retain autoantibodies with <0.20 coefficient of variation within each patient group and the controls, followed by *t* test for pairwise comparison of patients with CID, LS, and OS versus HDs to identify the top 50 targeted proteins, which were ranked on the basis of their *P* value and shown in Fig. 5A.

Autoantibodies against IFN-α, IFN-β, IFN-ω, IL-17A, IL-17F, IL-12, IL-22, and IL-23 were screened in 126 *RAG*-mutated patients (39 CID, 29 LS, 29 OS, and 29 SCID) and 43 HDs by a multiplex particle–based assay. Autoantibody neutralizing activity was assessed as previously described (*77*). The cutoff for positivity was defined as the means + 3 SD of the values obtained in HDs. Autoantibodies against IFN-λ were measured using a luciferase-based immunoprecipitation system as described (*78*).

### Tissue immunopathology

Skin biopsies from patients with OS and from patients with CID who have granulomatous lesions were analyzed by conventional immunohistochemistry and by RNAscope. For the latter, in situ hybridization for *IFNG*, *CXCL9*, and *CXCL10* on formalin-fixed paraffin-embedded samples was performed using the RNAscope 2.5 High-Definition BROWN Assay Kit (Advanced Cell Diagnostics, Newark, CA) according to the manufacturer's instructions (*79*). *POLR2A* mRNA labeling was used as positive control for the RNA quality in samples. The staining procedure was performed as described (*57*). T-bet (Abcam, catalog no. ab150440) (1:500) and GATA-3 (Roche, catalog no. 760-4897) (prediluted) protein expression was assessed by immunohistochemistry. Detection was performed on an automated immunostainer Benchmark Ultra (Roche) with the ultraView Universal DAB Detection Kit (catalog no. 760-500) or Ultra-View Universal AP Red Detection Kit (catalog no. 760-501). The detection kits were used independently (DAB, brown; AP, red). Images were taken with an Olympus Bx41 microscope, objective UPLanFI 10×/0.30, 20×/0.50∞/0.17, 40×/0.75∞/0.17, and 100×/1.30 oil with a U-TV0.5XC adaptor using an Olympus DP27 camera with an Olympus U-VTO.63XC adaptor, using CellSens, XV Image Processing imported into Adobe Photoshop CC 2024.

### Single-cell CITE-seq processing, sequencing, and clustering

Frozen PBMC samples from 11 *RAG*-mutated patients (P19, P21, and P27 with CID; P54 and P68 with LS; P88, P98, and P100 with OS; and P139, P140, and P141 with SCID) and seven HDs (three adult and four pediatric individuals) were thawed and processed as previously described for CITE-seq staining (*80*) and then subjected to single-cell RNA sequencing as described (*75*). Single-cell data processing, CITE-seq protein denoising and clustering, pseudobulk gene differential expression analysis, and gene set enrichment analysis (GSEA) were performed as described (*80*). Specifically, CellRanger (10x Genomics) version 6.0.1 was used to map cDNA libraries to the hg19 genome reference and to antibody tag barcodes. Data were further quality controlled and filtered using Seurat (v.4.1.1) (*81*) running in the R v4.2.1 environment. Upon filtering for single cells on the basis of demuxlet output, cells with fewer than 150 or more than 4000 detected genes, exceeding 30% mitochondrial reads, cell surface protein tag, or mRNA counts above 15,000 were excluded. The protein data underwent normalization and denoising using the double-strand break method (*82*). Clusters of major immune cell types were refined using RNA-based predicted cell type labels transferred from the Seurat Multimodal PBMC reference (*36*). Cell subset identification was further refined using integration with a reference PBMC dataset (*36*). Pseudobulk gene differential expression analysis and GSEA were performed as described (*80*). *P* values were adjusted using the Benjamini-Hochberg method for the whole gene set list.

### TCR and BCR data processing

CellRanger (10x Genomics) version 6.0.1 was used to create V(D)J contigs (*83*). Subsequently, the TCR and BCR sequence data were analyzed as described (*75*).

### Statistical analysis

For comparisons of two independent groups, the nonparametric Mann-Whitney *U* test was performed, and two-tailed *P* values below 0.05 were considered significant. For multiple comparisons, a one- or two-way nonparametric analysis of variance (Kruskal-Wallis *H* test) was applied, followed by Dunn's test to correct for multiple comparisons. For multiple comparisons, in which we compared grouped results, we used the mixed-effects model with Geisser-Greenhouse correction and Benjamini, Krieger, and Yekutieli's multiple comparisons test. Analysis of correlation between two parameters was done using the nonparametric Spearman test. Data graphs and analyses were generated using PRISM software (GraphPad Software Inc., v.10), and error bars display the SDs or SEMs, as indicated in each figure legend.

## Supplementary Materials

**The PDF file includes:**
Figs. S1 to S12
Tables S1 and S2
Legends for data files S1 to S11

**Other Supplementary Material for this manuscript includes the following:**
Data files S1 to S11
MDAR Reproducibility Checklist

## REFERENCES AND NOTES


1. M. A. Oettinger, D. G. Schatz, C. Gorka, D. Baltimore, RAG-1 and RAG-2, adjacent genes that synergistically activate V(D)J recombination. *Science* **248**, 1517–1523 (1990).
2. K. Schwarz, G. H. Gauss, L. Ludwig, U. Pannicke, Z. Li, D. Lindner, W. Friedrich, R. A. Seger, T. E. Hansen-Hagge, S. Desiderio, M. R. Lieber, C. R. Bartram, RAG mutations in human B cell-negative SCID. *Science* **274**, 97–99 (1996).
3. L. D. Notarangelo, M. S. Kim, J. E. Walter, Y. N. Lee, Human RAG mutations: Biochemistry and clinical implications. *Nat. Rev. Immunol.* **16**, 234–246 (2016).
4. H. IJspeert, G. J. Driessen, M. J. Moorhouse, N. G. Hartwig, B. Wolska-Kusnierz, K. Kalwak, A. Pituch-Noworolska, I. Kondratenko, J. M. van Montfrans, E. Mejstrikova, A. C. Lankester, A. W. Langerak, D. C. van Gent, A. P. Stubbs, J. J. M. van Dongen, M. van der Burg, Similar recombination-activating gene (RAG) mutations result in similar immunobiological effects but in different clinical phenotypes. *J. Allergy Clin. Immunol.* **133**, 1124–1133 (2014).
5. C. Schuetz, K. Huck, S. Gudowius, M. Megahed, O. Feyen, B. Hubner, D. T. Schneider, B. Manfras, U. Pannicke, R. Willemze, R. Knuchel, U. Gobel, A. Schulz, A. Borkhardt, W. Friedrich, K. Schwarz, T. Niehues, An immunodeficiency disease with RAG mutations and granulomas. *N. Engl. J. Med.* **358**, 2030–2038 (2008).
6. J. P. de Villartay, A. Lim, H. Al-Mousa, S. Dupont, J. Dechanet-Merville, E. Coumau-Gatbois, M. L. Gougeon, A. Lemainque, C. Eidenschenk, E. Jouanguy, L. Abel, J. L. Casanova, A. Fischer, F. Le Deist, A novel immunodeficiency associated with hypomorphic RAG1 mutations and CMV infection. *J. Clin. Invest.* **115**, 3291–3299 (2005).
7. S. Ehl, K. Schwarz, A. Enders, U. Duffner, U. Pannicke, J. Kuhr, F. Mascart, A. Schmitt-Graeff, C. Niemeyer, P. Fisch, A variant of SCID with specific immune responses and predominance of γδ T cells. *J. Clin. Invest.* **115**, 3140–3148 (2005).
8. O. M. Delmonte, C. Schuetz, L. D. Notarangelo, RAG deficiency: Two genes, many diseases. *J. Clin. Immunol.* **38**, 646–655 (2018).
9. M. S. Thakar, B. R. Logan, J. M. Puck, E. A. Dunn, R. H. Buckley, M. J. Cowan, R. J. O'Reilly, N. Kapoor, L. F. Satter, S. Y. Pai, J. Heimall, S. Chandra, C. L. Ebens, D. Chellapandian, O. Williams, L. M. Burroughs, B. D. Saldana, A. Rayes, L. M. Madden, S. Chandrakasan, J. J. Bednarski II, K. B. DeSantes, G. D. E. Cuvelier, P. Teira, A. P. Gillio, H. Eissa, A. P. Knutsen, F. D. Goldman, V. M. Aquino, E. B. Shereck, T. B. Moore, E. H. Caywood, M. T. V. Lugt, J. Rozmus, L. Broglie, L. C. Yu, A. J. Shah, J. R. Andolina, X. Liu, R. E. Parrott, J. Dara, S. Prockop, C. A. Martinez, M. Kapadia, S. C. Jyonouchi, K. E. Sullivan, J. J. Bleesing, S. Chaudhury, A. Petrovic, M. D. Keller, T. C. Quigg, S. Parikh, S. Shenoy, C. Seroogy, T. Rubin, H. Decaluwe, J. M. Routes, T. R. Torgerson, J. W. Leiding, M. A. Pulsipher, D. B. Kohn, L. M. Griffith, E. Haddad, C. C. Dvorak, L. D. Notarangelo, Measuring the effect of newborn screening on survival after haematopoietic cell transplantation for severe combined immunodeficiency: A 36-year longitudinal study from the Primary Immune Deficiency Treatment Consortium. *Lancet* **402**, 129–140 (2023).
10. C. Schuetz, J. Gerke, M. Ege, J. Walter, M. Kusters, A. Worth, J. A. Kanakry, D. Dimitrova, B. Wolska-Kusnierz, K. Chen, E. Unal, M. Karakukcu, O. Pashchenko, J. Leiding, T. Kawai, P. J. Amrolia, D. Berghuis, J. Buechner, D. Buchbinder, M. J. Cowan, A. R. Gennery, T. Gungor, J. Heimall, M. Miano, I. Meyts, E. C. Morris, J. Riviere, S. O. Sharapova, P. J. Shaw, M. Slatter, M. Honig, P. Veys, A. Fischer, M. Cavazzana, D. Moshous, A. Schulz, M. H. Albert, J. M. Puck, A. C. Lankester, L. D. Notarangelo, B. Neven, Hypomorphic RAG deficiency: Impact of disease burden on survival and thymic recovery argues for early diagnosis and HSCT. *Blood* **141**, 713–724 (2023).
11. Y. N. Lee, F. Frugoni, K. Dobbs, J. E. Walter, S. Giliani, A. R. Gennery, W. Al-Herz, E. Haddad, F. LeDeist, J. H. Bleesing, L. A. Henderson, S. Y. Pai, R. P. Nelson, D. H. El-Ghoneimy, R. A. El-Feky, S. M. Reda, E. Hossny, P. Soler-Palacin, R. L. Fuleihan, N. C. Patel, M. J. Massaad, R. S. Geha, J. M. Puck, P. Palma, C. Cancrini, K. Chen, M. Vihinen, F. W. Alt, L. D. Notarangelo, A systematic analysis of recombination activity and genotype-phenotype correlation in human recombination-activating gene 1 deficiency. *J. Allergy Clin. Immunol.* **133**, 1099–1108.e12 (2014).
12. I. Tirosh, Y. Yamazaki, F. Frugoni, F. A. Ververs, E. J. Allenspach, Y. Zhang, S. Burns, W. Al-Herz, L. Noroski, J. E. Walter, A. R. Gennery, M. van der Burg, L. D. Notarangelo, Y. N. Lee, Recombination activity of human recombination-activating gene 2 (RAG2) mutations and correlation with clinical phenotype. *J. Allergy Clin. Immunol.* **143**, 726–735 (2019).
13. C. S. Seet, C. He, M. T. Bethune, S. Li, B. Chick, E. H. Gschweng, Y. Zhu, K. Kim, D. B. Kohn, D. Baltimore, G. M. Crooks, A. Montel-Hagen, Generation of mature T cells from human hematopoietic stem and progenitor cells in artificial thymic organoids. *Nat. Methods* **14**, 521–530 (2017).
14. M. Bosticardo, F. Pala, E. Calzoni, O. M. Delmonte, K. Dobbs, C. L. Gardner, N. Sacchetti, T. Kawai, E. K. Garabedian, D. Draper, J. R. E. Bergerson, S. S. DeRavin, A. F. Freeman, T. Gungor, N. Hartog, S. M. Holland, D. B. Kohn, H. L. Malech, M. L. Markert, K. G. Weinacht, A. Villa, C. S. Seet, A. Montel-Hagen, G. M. Crooks, L. D. Notarangelo, Artificial thymic organoids represent a reliable tool to study T-cell differentiation in patients with severe T-cell lymphopenia. *Blood Adv.* **4**, 2611–2616 (2020).
15. A. Berland, J. Rosain, S. Kaltenbach, V. Allain, N. Mahlaoui, I. Melki, A. Fievet, C. Dubois d'Enghien, M. Ouachee-Chardin, L. Perrin, N. Auger, F. E. Cipe, A. Finocchi, F. Dogu, F. Suarez, D. Moshous, T. Leblanc, A. Belot, C. Fieschi, D. Boutboul, M. Malphettes, L. Galicier, E. Oksenhendler, S. Blanche, A. Fischer, P. Revy, D. Stoppa-Lyonnet, C. Picard, J. P. de Villartay, PROMIDISα: A T-cell receptor α signature associated with immunodeficiencies caused by V(D)J recombination defects. *J. Allergy Clin. Immunol.* **143**, 325–334.e2 (2019).
16. J. M. Moreau, V. Gouirand, M. D. Rosenblum, T-cell adhesion in healthy and inflamed skin. *JID Innov.* **1**, 100014 (2021).
17. S. Becattini, D. Latorre, F. Mele, M. Foglierini, C. De Gregorio, A. Cassotta, B. Fernandez, S. Kelderman, T. N. Schumacher, D. Corti, A. Lanzavecchia, F. Sallusto, T cell immunity. Functional heterogeneity of human memory $CD4^+$ T cell clones primed by pathogens or vaccines. *Science* **347**, 400–406 (2015).
18. A. Pivarcsi, M. Gombert, M. C. Dieu-Nosjean, A. Lauerma, R. Kubitza, S. Meller, J. Rieker, A. Muller, L. Da Cunha, A. Haahtela, E. Sonkoly, W. H. Fridman, H. Alenius, L. Kemeny, T. Ruzicka, A. Zlotnik, B. Homey, CC chemokine ligand 18, an atopic dermatitis-associated and dendritic cell-derived chemokine, is regulated by staphylococcal products and allergen exposure. *J. Immunol.* **173**, 5810–5817 (2004).
19. C. S. Kaetzel, The polymeric immunoglobulin receptor: Bridging innate and adaptive immune responses at mucosal surfaces. *Immunol. Rev.* **206**, 83–99 (2005).
20. J. E. Walter, F. Rucci, L. Patrizi, M. Recher, S. Regenass, T. Paganini, M. Keszei, I. Pessach, P. A. Lang, P. L. Poliani, S. Giliani, W. Al-Herz, M. J. Cowan, J. M. Puck, J. Bleesing, T. Niehues, C. Schuetz, H. Malech, S. S. DeRavin, F. Facchetti, A. R. Gennery, E. Andersson, N. R. Kamani, J. Sekiguchi, H. M. Alenezi, J. Chinen, G. Dbaibo, G. ElGhazali, A. Fontana, S. Pasic, C. Detre, C. Terhorst, F. W. Alt, L. D. Notarangelo, Expansion of immunoglobulin-secreting cells and defects in B cell tolerance in Rag-dependent immunodeficiency. *J. Exp. Med.* **207**, 1541–1554 (2010).
21. B. Cassani, P. L. Poliani, V. Marrella, F. Schena, A. V. Sauer, M. Ravanini, D. Strina, C. E. Busse, S. Regenass, H. Wardemann, A. Martini, F. Facchetti, M. van der Burg, A. G. Rolink, P. Vezzoni, F. Grassi, E. Traggiai, A. Villa, Homeostatic expansion of autoreactive immunoglobulin-secreting cells in the Rag2 mouse model of Omenn syndrome. *J. Exp. Med.* **207**, 1525–1540 (2010).
22. K. Csomos, B. Ujhazi, P. Blazso, J. L. Herrera, C. M. Tipton, T. Kawai, S. Gordon, M. Ellison, K. Wu, M. Stowell, L. Haynes, R. Cruz, B. Zakota, J. Nguyen, M. Altrich, C. B. Geier, S. Sharapova, J. F. Dasso, J. W. Leiding, G. Smith, W. Al-Herz, M. de Barros Dorna, O. Fadugba, E. Fronkova, V. Kanderova, M. Svaton, S. E. Henrickson, J. D. Hernandez, T. Kuijpers, S. M. Kandilarova, E. Naumova, T. Milota, A. Sediva, D. Moshous, B. Neven, T. Saco, R. Sargur, S. Savic, J. Sleasman, G. Sunkersett, B. R. Ward, M. Komatsu, S. Pittaluga, A. Kumanovics, M. J. Butte, M. P. Cancro, S. Pillai, E. Meffre, L. D. Notarangelo, J. E. Walter, Partial RAG deficiency in humans induces dysregulated peripheral lymphocyte development and humoral tolerance defect with accumulation of T-$bet^+$ B cells. *Nat. Immunol.* **23**, 1256–1272 (2022).
23. A. S. Wolff, J. Karner, J. F. Owe, B. E. Oftedal, N. E. Gilhus, M. M. Erichsen, O. Kampe, A. Meager, P. Peterson, K. Kisand, N. Willcox, E. S. Husebye, Clinical and serologic parallels to APS-I in patients with thymomas and autoantigen transcripts in their tumors. *J. Immunol.* **193**, 3880–3890 (2014).
24. E. M. N. Ferre, T. J. Break, P. D. Burbelo, M. Allgauer, D. E. Kleiner, D. Jin, Z. Xu, L. R. Folio, D. J. Mollura, M. Swamydas, W. Gu, S. Hunsberger, C. R. Lee, A. Bondici, K. W. Hoffman, J. K. Lim, K. Dobbs, J. E. Niemela, T. A. Fleisher, A. P. Hsu, L. N. Snow, D. N. Darnell, S. Ojaimi, M. A. Cooper, M. Bozzola, G. I. Kleiner, J. C. Martinez, R. R. Deterding, D. B. Kuhns, T. Heller, K. K. Winer, A. Rajan, S. M. Holland, L. D. Notarangelo, K. P. Fennelly, K. N. Olivier, M. S. Lionakis, Lymphocyte-driven regional immunopathology in pneumonitis caused by impaired central immune tolerance. *Sci. Transl. Med.* **11**, eaav5597 (2019).
25. P. Holla, B. Dizon, A. A. Ambegaonkar, N. Rogel, E. Goldschmidt, A. K. Boddapati, H. Sohn, D. Sturdevant, J. W. Austin, L. Kardava, L. Yuesheng, P. Liu, S. Moir, S. K. Pierce, A. Madi, Shared transcriptional profiles of atypical B cells suggest common drivers of expansion and function in malaria, HIV, and autoimmunity. *Sci. Adv.* **7**, eabg8384 (2021).
26. A. H. Ellebedy, K. J. Jackson, H. T. Kissick, H. I. Nakaya, C. W. Davis, K. M. Roskin, A. K. McElroy, C. M. Oshansky, R. Elbein, S. Thomas, G. M. Lyon, C. F. Spiropoulou, A. K. Mehta, P. G. Thomas, S. D. Boyd, R. Ahmed, Defining antigen-specific plasmablast and memory B cell subsets in human blood after viral infection or vaccination. *Nat. Immunol.* **17**, 1226–1234 (2016).
27. C. M. Tipton, C. F. Fucile, J. Darce, A. Chida, T. Ichikawa, I. Gregoretti, S. Schieferl, J. Hom, S. Jenks, R. J. Feldman, R. Mehr, C. Wei, F. E. Lee, W. C. Cheung, A. F. Rosenberg, I. Sanz,

Diversity, cellular origin and autoreactivity of antibody-secreting cell population expansions in acute systemic lupus erythematosus. *Nat. Immunol.* **16**, 755–765 (2015).
28. I. Sanz, C. Wei, S. A. Jenks, K. S. Cashman, C. Tipton, M. C. Woodruff, J. Hom, F. E. Lee, Challenges and opportunities for consistent classification of human B cell and plasma cell populations. *Front. Immunol.* **10**, 2458 (2019).
29. B. Keller, V. Strohmeier, I. Harder, S. Unger, K. J. Payne, G. Andrieux, M. Boerries, P. T. Felixberger, J. J. M. Landry, A. Nieters, A. Rensing-Ehl, U. Salzer, N. Frede, S. Usadel, R. Elling, C. Speckmann, I. Hainmann, E. Ralph, K. Gilmour, M. W. J. Wentink, M. van der Burg, H. S. Kuehn, S. D. Rosenzweig, U. Kolsch, H. von Bernuth, P. Kaiser-Labusch, F. Gothe, S. Hambleton, A. D. Vlagea, A. Garcia Garcia, L. Alsina, G. Markelj, T. Avcin, J. Vasconcelos, M. Guedes, J. Y. Ding, C. L. Ku, B. Shadur, D. T. Avery, N. Venhoff, J. Thiel, H. Becker, L. Erazo-Borras, C. M. Trujillo-Vargas, J. L. Franco, C. Fieschi, S. Okada, P. E. Gray, G. Uzel, J. L. Casanova, M. Fliegauf, B. Grimbacher, H. Eibel, S. Ehl, R. E. Voll, M. Rizzi, P. Stepensky, V. Benes, C. S. Ma, C. Bossen, S. G. Tangye, K. Warnatz, The expansion of human T-bet$^{high}$CD21$^{low}$ B cells is T cell dependent. *Sci. Immunol.* **6**, eabh0891 (2021).
30. S. G. Tangye, Do multiple subsets of CD11c$^{+}$ B cells exist? You (T)-Bet! *J. Allergy Clin. Immunol.* **152**, 607–609 (2023).
31. F. K. Stevenson, M. Wrightham, M. J. Glennie, D. B. Jones, A. R. Cattan, T. Feizi, T. J. Hamblin, G. T. Stevenson, Antibodies to shared idiotypes as agents for analysis and therapy for human B cell tumors. *Blood* **68**, 430–436 (1986).
32. V. Pascual, K. Victor, D. Lelsz, M. B. Spellerberg, T. J. Hamblin, K. M. Thompson, I. Randen, J. Natvig, J. D. Capra, F. K. Stevenson, Nucleotide sequence analysis of the V regions of two IgM cold agglutinins. Evidence that the VH4-21 gene segment is responsible for the major cross-reactive idiotype. *J. Immunol.* **146**, 4385–4391 (1991).
33. K. N. Potter, Y. Li, V. Pascual, R. C. Williams Jr., L. C. Byres, M. Spellerberg, F. K. Stevenson, J. D. Capra, Molecular characterization of a cross-reactive idiotope on human immunoglobulins utilizing the VH4-21 gene segment. *J. Exp. Med.* **178**, 1419–1428 (1993).
34. J. N. Schickel, S. Glauzy, Y. S. Ng, N. Chamberlain, C. Massad, I. Isnardi, N. Katz, G. Uzel, S. M. Holland, C. Picard, A. Puel, J. L. Casanova, E. Meffre, Self-reactive VH4-34-expressing IgG B cells recognize commensal bacteria. *J. Exp. Med.* **214**, 1991–2003 (2017).
35. A. J. Cappione, A. E. Pugh-Bernard, J. H. Anolik, I. Sanz, Lupus IgG VH4.34 antibodies bind to a 220-kDa glycoform of CD45/B220 on the surface of human B lymphocytes. *J. Immunol.* **172**, 4298–4307 (2004).
36. Y. Hao, S. Hao, E. Andersen-Nissen, W. M. Mauck III, S. Zheng, A. Butler, M. J. Lee, A. J. Wilk, C. Darby, M. Zager, P. Hoffman, M. Stoeckius, E. Papalexi, E. P. Mimitou, J. Jain, A. Srivastava, T. Stuart, L. M. Fleming, B. Yeung, A. J. Rogers, J. M. McElrath, C. A. Blish, R. Gottardo, P. Smibert, R. Satija, Integrated analysis of multimodal single-cell data. *Cell* **184**, 3573–3587.e29 (2021).
37. M. E. Cook, T. R. Bradstreet, A. M. Webber, J. Kim, A. Santeford, K. M. Harris, M. K. Murphy, J. Tran, N. M. Abdalla, E. A. Schwarzkopf, S. C. Greco, C. M. Halabi, R. S. Apte, P. J. Blackshear, B. T. Edelson, The ZFP36 family of RNA binding proteins regulates homeostatic and autoreactive T cell responses. *Sci. Immunol.* **7**, eabo0981 (2022).
38. L. M. Paardekooper, M. B. Bendix, A. Ottria, L. W. de Haer, M. Ter Beest, T. Radstake, W. Marut, G. van den Bogaart, Hypoxia potentiates monocyte-derived dendritic cells for release of tumor necrosis factor α via MAP3K8. *Biosci. Rep.* **38**, BSR20182019 (2018).
39. X. B. Ling, H. W. Wei, J. Wang, Y. Q. Kong, Y. Y. Wu, J. L. Guo, T. F. Li, J. K. Li, Mammalian metallothionein-2A and oxidative stress. *Int. J. Mol. Sci.* **17**, 1483 (2016).
40. S. Kano, K. Sato, Y. Morishita, S. Vollstedt, S. Kim, K. Bishop, K. Honda, M. Kubo, T. Taniguchi, The contribution of transcription factor IRF1 to the interferon-γ-interleukin 12 signaling axis and TH1 versus TH-17 differentiation of CD4$^{+}$ T cells. *Nat. Immunol.* **9**, 34–41 (2008).
41. M. A. Toscano, G. A. Bianco, J. M. Ilarregui, D. O. Croci, J. Correale, J. D. Hernandez, N. W. Zwirner, F. Poirier, E. M. Riley, L. G. Baum, G. A. Rabinovich, Differential glycosylation of TH1, TH2 and TH-17 effector cells selectively regulates susceptibility to cell death. *Nat. Immunol.* **8**, 825–834 (2007).
42. S. Bruhn, Y. Fang, F. Barrenas, M. Gustafsson, H. Zhang, A. Konstantinell, A. Kronke, B. Sonnichsen, A. Bresnick, N. Dulyaninova, H. Wang, Y. Zhao, J. Klingelhofer, N. Ambartsumian, M. K. Beck, C. Nestor, E. Bona, Z. Xiang, M. Benson, A generally applicable translational strategy identifies S100A4 as a candidate gene in allergy. *Sci. Transl. Med.* **6**, 218ra4 (2014).
43. G. Bixel, S. Kloep, S. Butz, B. Petri, B. Engelhardt, D. Vestweber, Mouse CD99 participates in T-cell recruitment into inflamed skin. *Blood* **104**, 3205–3213 (2004).
44. T. Shea-Donohue, A. Zhao, T. M. Antalis, SerpinB2 mediated regulation of macrophage function during enteric infection. *Gut Microbes* **5**, 254–258 (2014).
45. J. Ha, M. Kim, J. S. Park, Y. Lee, J. Y. Lee, J. C. Shin, D. Seo, S. S. Park, J. You, S. M. Jung, H. Y. Kim, S. Mizuno, S. Takahashi, S. J. Kim, S. H. Park, SERTAD1 initiates NLRP3-mediated inflammasome activation through restricting NLRP3 polyubiquitination. *Cell Rep.* **43**, 113752 (2024).
46. P. Mombaerts, J. Iacomini, R. S. Johnson, K. Herrup, S. Tonegawa, V. E. Papaioannou, RAG-1-deficient mice have no mature B and T lymphocytes. *Cell* **68**, 869–877 (1992).
47. Y. Shinkai, G. Rathbun, K. P. Lam, E. M. Oltz, V. Stewart, M. Mendelsohn, J. Charron, M. Datta, F. Young, A. M. Stall, F. W. Alt, RAG-2-deficient mice lack mature lymphocytes owing to inability to initiate V(D)J rearrangement. *Cell* **68**, 855–867 (1992).
48. E. Haddad, B. R. Logan, L. M. Griffith, R. H. Buckley, R. E. Parrott, S. E. Prockop, T. N. Small, J. Chaisson, C. C. Dvorak, M. Murnane, N. Kapoor, H. Abdel-Azim, I. C. Hanson, C. Martinez, J. J. H. Bleesing, S. Chandra, A. R. Smith, M. E. Cavanaugh, S. Jyonouchi, K. E. Sullivan, L. Burroughs, S. Skoda-Smith, A. E. Haight, A. G. Tumlin, T. C. Quigg, C. Taylor, B. J. D. Saldana, M. D. Keller, C. M. Seroogy, K. B. Desantes, A. Petrovic, J. W. Leiding, D. C. Shyr, H. Decaluwe, P. Teira, A. P. Gillio, A. P. Knutsen, T. B. Moore, M. Kletzel, J. A. Craddock, V. Aquino, J. H. Davis, L. C. Yu, G. D. E. Cuvelier, J. J. Bednarski, F. D. Goldman, E. M. Kang, E. Shereck, M. H. Porteus, J. A. Connelly, T. A. Fleisher, H. L. Malech, W. T. Shearer, P. Szabolcs, M. S. Thakar, M. T. V. Lugt, J. Heimall, Z. Yin, M. A. Pulsipher, S. Y. Pai, D. B. Kohn, J. M. Puck, M. J. Cowan, R. J. O'Reilly, L. D. Notarangelo, SCID genotype and 6-month posttransplant CD4 count predict survival and immune recovery. *Blood* **132**, 1737–1749 (2018).
49. M. J. Ege, C. Schuetz, E. M. Jacobsen, S. M. Muller-Langer, I. Furlan, M. Sirin, U. Pannicke, K. Schwarz, K. M. Debatin, M. Honig, A. Schulz, W. Friedrich, Late thymic deficiency after HLA-haploidentical hematopoietic stem cell transplantation for severe combined immunodeficiency. *J. Allergy Clin. Immunol.* **143**, 1623–1626.e13 (2019).
50. H. Yoshida, C. A. Lareau, R. N. Ramirez, S. A. Rose, B. Maier, A. Wroblewska, F. Desland, A. Chudnovskiy, A. Mortha, C. Dominguez, J. Tellier, E. Kim, D. Dwyer, S. Shinton, T. Nabekura, Y. Qi, B. Yu, M. Robinette, K. W. Kim, A. Wagers, A. Rhoads, S. L. Nutt, B. D. Brown, S. Mostafavi, J. D. Buenrostro, C. Benoist, Immunological Genome Project, The cis-regulatory atlas of the mouse immune system. *Cell* **176**, 897–912.e20 (2019).
51. A. K. Naik, D. J. Dauphars, E. Corbett, L. Simpson, D. G. Schatz, M. S. Krangel, RORγt up-regulates RAG gene expression in DP thymocytes to expand the Tcra repertoire. *Sci. Immunol.* **9**, eadh5318 (2024).
52. L. Schandene, A. Ferster, F. Mascart-Lemone, A. Crusiaux, C. Gerard, A. Marchant, M. Lybin, T. Velu, E. Sariban, M. Goldman, T helper type 2-like cells and therapeutic effects of interferon-gamma in combined immunodeficiency with hypereosinophilia (Omenn's syndrome). *Eur. J. Immunol.* **23**, 56–60 (1993).
53. D. R. Wesemann, J. M. Magee, C. Boboila, D. P. Calado, M. P. Gallagher, A. J. Portuguese, J. P. Manis, X. Zhou, M. Recher, K. Rajewsky, L. D. Notarangelo, F. W. Alt, Immature B cells preferentially switch to IgE with increased direct Sμ to Sε recombination. *J. Exp. Med.* **208**, 2733–2746 (2011).
54. O. Yoshie, K. Matsushima, CCR4 and its ligands: From bench to bedside. *Int. Immunol.* **27**, 11–20 (2015).
55. Y. Mitamura, M. Reiger, J. Kim, Y. Xiao, D. Zhakparov, G. Tan, B. Ruckert, A. O. Rinaldi, K. Baerenfaller, M. Akdis, M. C. Bruggen, K. C. Nadeau, P. M. Brunner, D. Roqueiro, C. Traidl-Hoffmann, C. A. Akdis, Spatial transcriptomics combined with single-cell RNA-sequencing unravels the complex inflammatory cell network in atopic dermatitis. *Allergy* **78**, 2215–2231 (2023).
56. E. Guttman-Yassky, R. Bissonnette, B. Ungar, M. Suarez-Farinas, M. Ardeleanu, H. Esaki, M. Suprun, Y. Estrada, H. Xu, X. Peng, J. I. Silverberg, A. Menter, J. G. Krueger, R. Zhang, U. Chaudhry, B. Swanson, N. M. H. Graham, G. Pirozzi, G. D. Yancopoulos, J. D. D. Hamilton, Dupilumab progressively improves systemic and cutaneous abnormalities in patients with atopic dermatitis. *J. Allergy Clin. Immunol.* **143**, 155–172 (2019).
57. R. Rigoni, E. Fontana, K. Dobbs, V. Marrella, V. Taverniti, V. Maina, A. Facoetti, G. D'Amico, W. Al-Herz, M. E. Cruz-Munoz, C. Schuetz, A. R. Gennery, E. K. Garabedian, S. Giliani, D. Draper, G. Dbaibo, R. S. Geha, I. Meyts, T. Tousseyn, B. Neven, D. Moshous, A. Fischer, A. Schulz, A. Finocchi, D. B. Kuhns, D. L. Fink, M. S. Lionakis, M. Swamydas, S. Guglielmetti, J. Alejo, I. A. Myles, S. Pittaluga, L. D. Notarangelo, A. Villa, B. Cassani, Cutaneous barrier leakage and gut inflammation drive skin disease in Omenn syndrome. *J. Allergy Clin. Immunol.* **146**, 1165–1179.e11 (2020).
58. R. Rigoni, E. Fontana, S. Guglielmetti, B. Fosso, A. M. D'Erchia, V. Maina, V. Taverniti, M. C. Castiello, S. Mantero, G. Pacchiana, S. Musio, R. Pedotti, C. Selmi, J. R. Mora, G. Pesole, P. Vezzoni, P. L. Poliani, F. Grassi, A. Villa, B. Cassani, Intestinal microbiota sustains inflammation and autoimmunity induced by hypomorphic RAG defects. *J. Exp. Med.* **213**, 355–375 (2016).
59. E. L. Simpson, T. Bieber, E. Guttman-Yassky, L. A. Beck, A. Blauvelt, M. J. Cork, J. I. Silverberg, M. Deleuran, Y. Kataoka, J. P. Lacour, K. Kingo, M. Worm, Y. Poulin, A. Wollenberg, Y. Soo, N. M. Graham, G. Pirozzi, B. Akinlade, H. Staudinger, V. Mastey, L. Eckert, A. Gadkari, N. Stahl, G. D. Yancopoulos, M. Ardeleanu, SOLO 1 and SOLO 2 Investigators, Two phase 3 trials of dupilumab versus placebo in atopic dermatitis. *N. Engl. J. Med.* **375**, 2335–2348 (2016).
60. T. Ahn, G. Sheng, M. Garcia-Lloret, M. Butte, A proposed targeted treatment for Omenn syndrome – A case report. *J. Clin. Immunol.* **41**, 113–115 (2021).
61. B. Neven, P. Perot, J. Bruneau, M. Pasquet, M. Ramirez, J. S. Diana, S. Luzi, N. Corre-Catelin, C. Chardot, D. Moshous, S. Leclerc Mercier, N. Mahlaoui, N. Aladjidi, B. Le Bail, M. Lecuit, C. Bodemer, T. J. Molina, S. Blanche, M. Eloit, Cutaneous and visceral chronic granulomatous disease triggered by a rubella virus vaccine strain in children with primary immunodeficiencies. *Clin. Infect. Dis.* **64**, 83–86 (2017).
62. L. Perelygina, J. Icenogle, K. E. Sullivan, Rubella virus-associated chronic inflammation in primary immunodeficiency diseases. *Curr. Opin. Allergy Clin. Immunol.* **20**, 574–581 (2020).
63. J. R. Farmer, Z. Foldvari, B. Ujhazi, S. S. De Ravin, K. Chen, J. J. H. Bleesing, C. Schuetz, W. Al-Herz, R. S. Abraham, A. Y. Joshi, B. T. Costa-Carvalho, D. Buchbinder, C. Booth,

A. Reiff, P. J. Ferguson, A. Aghamohammadi, H. Abolhassani, J. M. Puck, M. Adeli, C. Cancrini, P. Palma, A. Bertaina, F. Locatelli, G. Di Matteo, R. S. Geha, M. G. Kanariou, L. Lycopoulou, M. Tzanoudaki, J. W. Sleasman, S. Parikh, G. Pinero, B. M. Fischer, G. Dbaibo, E. Unal, T. Patiroglu, M. Karakukcu, K. K. Al-Saad, M. A. Dilley, S. Y. Pai, C. M. Dutmer, E. W. Gelfand, C. B. Geier, M. M. Eibl, H. M. Wolf, L. A. Henderson, M. M. Hazen, C. Bonfim, B. Wolska-Kusnierz, M. J. Butte, J. D. Hernandez, S. K. Nicholas, P. Stepensky, S. Chandrakasan, M. Miano, E. Westermann-Clark, V. Goda, G. Krivan, S. M. Holland, O. Fadugba, S. E. Henrickson, A. Ozen, E. Karakoc-Aydiner, S. Baris, A. Kiykim, R. Bredius, B. Hoeger, K. Boztug, O. Pashchenko, B. Neven, D. Moshous, J. P. Villartay, A. A. Bousfiha, H. R. Hill, L. D. Notarangelo, J. E. Walter, Outcomes and treatment strategies for autoimmunity and hyperinflammation in patients with RAG deficiency. *J. Allergy Clin. Immunol. Pract.* **7**, 1970–1985.e4 (2019).

64. S. E. Vazquez, S. A. Mann, A. Bodansky, A. F. Kung, Z. Quandt, E. M. N. Ferre, N. Landegren, D. Eriksson, P. Bastard, S. Y. Zhang, J. Liu, A. Mitchell, I. Proekt, D. Yu, C. Mandel-Brehm, C. Y. Wang, B. Miao, G. Sowa, K. Zorn, A. Y. Chan, V. M. Tagi, C. Shimizu, A. Tremoulet, K. Lynch, M. R. Wilson, O. Kampe, K. Dobbs, O. M. Delmonte, R. Bacchetta, L. D. Notarangelo, J. C. Burns, J. L. Casanova, M. S. Lionakis, T. R. Torgerson, M. S. Anderson, J. L. DeRisi, Autoantibody discovery across monogenic, acquired, and COVID-19-associated autoimmunity with scalable PhIP-seq. *eLife* **11**, e78550 (2022).
65. C. N. Miller, M. R. Waterfield, J. M. Gardner, M. S. Anderson, Aire in autoimmunity. *Annu. Rev. Immunol.* **42**, 427–453 (2024).
66. T. Le Voyer, A. V. Parent, X. Liu, A. Cederholm, A. Gervais, J. Rosain, T. Nguyen, M. P. Lorenzo, E. Rackaityte, D. Rinchai, P. Zhang, L. Bizien, G. Hancioglu, P. Ghillani-Dalbin, J. L. Charuel, Q. Philippot, M. S. Gueye, M. R. L. Maglorius Renkilaraj, M. Ogishi, C. Soudee, M. Migaud, F. Rozenberg, M. Momenilandi, Q. Riller, L. Imberti, O. M. Delmonte, G. Muller, B. Keller, J. Orrego, W. A. F. Gallego, T. Rubin, M. Emiroglu, N. Parvaneh, D. Eriksson, M. Aranda-Guillen, D. I. Berrios, L. Vong, C. H. Katelaris, P. Mustillo, J. Raedler, J. Bohlen, J. B. Celik, C. Astudillo, S. Winter, NF-κB Consortium, C. H. G. Effort, C. McLean, A. Guffroy, J. L. DeRisi, D. Yu, C. Miller, Y. Feng, A. Guichard, V. Beziat, J. Bustamante, Q. Pan-Hammarstrom, Y. Zhang, L. B. Rosen, S. M. Holland, M. Bosticardo, H. Kenney, R. Castagnoli, C. A. Slade, K. Boztug, N. Mahlaoui, S. Latour, R. S. Abraham, V. Lougaris, F. Hauck, A. Sediva, F. Atschekzei, G. Sogkas, M. C. Poli, M. A. Slatter, B. Palterer, M. D. Keller, A. Pinzon-Charry, A. Sullivan, L. Droney, D. Suan, M. Wong, A. Kane, H. Hu, C. Ma, H. Grombirikova, P. Ciznar, I. Dalal, N. Aladjidi, M. Hie, E. Lazaro, J. Franco, S. Keles, M. Malphettes, M. Pasquet, M. E. Maccari, A. Meinhardt, A. Ikinciogullari, M. Shahrooei, F. Celmeli, P. Frosk, C. C. Goodnow, P. E. Gray, A. Belot, H. S. Kuehn, S. D. Rosenzweig, M. Miyara, F. Licciardi, A. Servettaz, V. Barlogis, G. Le Guenno, V. M. Herrmann, T. Kuijpers, G. Ducoux, F. Sarrot-Reynauld, C. Schuetz, C. Cunningham-Rundles, F. Rieux-Laucat, S. G. Tangye, C. Sobacchi, R. Doffinger, K. Warnatz, B. Grimbacher, C. Fieschi, L. Berteloot, V. L. Bryant, S. T. Assant, H. Su, B. Neven, L. Abel, Q. Zhang, B. Boisson, A. Cobat, E. Jouanguy, O. Kampe, P. Bastard, C. M. Roifman, N. Landegren, L. D. Notarangelo, M. S. Anderson, J. L. Casanova, A. Puel, Autoantibodies against type I IFNs in humans with alternative NF-κB pathway deficiency. *Nature* **623**, 803–813 (2023).
67. T. Akiyama, Y. Shimo, H. Yanai, J. Qin, D. Ohshima, Y. Maruyama, Y. Asaumi, J. Kitazawa, H. Takayanagi, J. M. Penninger, M. Matsumoto, T. Nitta, Y. Takahama, J. Inoue, The tumor necrosis factor family receptors RANK and CD40 cooperatively establish the thymic medullary microenvironment and self-tolerance. *Immunity* **29**, 423–437 (2008).
68. P. Cavadini, W. Vermi, F. Facchetti, S. Fontana, S. Nagafuchi, E. Mazzolari, A. Sediva, V. Marrella, A. Villa, A. Fischer, L. D. Notarangelo, R. Badolato, AIRE deficiency in thymus of 2 patients with Omenn syndrome. *J. Clin. Invest.* **115**, 728–732 (2005).
69. S. S. De Ravin, E. W. Cowen, K. A. Zarember, N. L. Whiting-Theobald, D. B. Kuhns, N. G. Sandler, D. C. Douek, S. Pittaluga, P. L. Poliani, Y. N. Lee, L. D. Notarangelo, L. Wang, F. W. Alt, E. M. Kang, J. D. Milner, J. E. Niemela, M. Fontana-Penn, S. H. Sinal, H. L. Malech, Hypomorphic Rag mutations can cause destructive midline granulomatous disease. *Blood* **116**, 1263–1271 (2010).
70. J. H. Rowe, B. D. Stadinski, L. A. Henderson, L. Ott de Bruin, O. Delmonte, Y. N. Lee, M. T. de la Morena, R. K. Goyal, A. Hayward, C. H. Huang, M. Kanariou, A. King, T. W. Kuijpers, J. Y. Soh, B. Neven, J. E. Walter, E. S. Huseby, L. D. Notarangelo, Abnormalities of T-cell receptor repertoire in $CD4^+$ regulatory and conventional T cells in patients with RAG mutations: Implications for autoimmunity. *J. Allergy Clin. Immunol.* **140**, 1739–1743. e7 (2017).
71. P. Bastard, L. B. Rosen, Q. Zhang, E. Michailidis, H.-H. Hoffmann, Y. Zhang, K. Dorgham, Q. Philippot, J. Rosain, V. Béziat, J. Manry, E. Shaw, L. Haljasmägi, P. Peterson, L. Lorenzo, L. Bizien, S. Trouillet-Assant, K. Dobbs, A. A. de Jesus, A. Belot, A. Kallaste, E. Catherinot, Y. Tandjaoui-Lambiotte, J. L. Pen, G. Kerner, B. Bigio, Y. Seeleuthner, R. Yang, A. Bolze, A. N. Spaan, O. M. Delmonte, M. S. Abers, A. Aiuti, G. Casari, V. Lampasona, L. Piemonti, F. Ciceri, K. Bilguvar, R. P. Lifton, M. Vasse, D. M. Smadja, M. Migaud, J. Hadjadj, B. Terrier, D. Duffy, L. Quintana-Murci, D. van de Beek, L. Roussel, D. C. Vinh, S. G. Tangye, F. Haerynck, D. Dalmau, J. Martinez-Picado, P. Brodin, M. C. Nussenzweig, S. Boisson-Dupuis, C. Rodríguez-Gallego, G. Vogt, T. H. Mogensen, A. J. Oler, J. Gu, P. D. Burbelo, J. I. Cohen, A. Biondi, L. R. Bettini, M. D'Angio, P. Bonfanti, P. Rossignol, J. Mayaux, F. Rieux-Laucat, E. S. Husebye, F. Fusco, M. V. Ursini, L. Imberti, A. Sottini, S. Paghera, E. Quiros-Roldan, C. Rossi, R. Castagnoli, D. Montagna, A. Licari, G. L. Marseglia, X. Duval, J. Ghosn, HGID Lab, NIAID-USUHS Immune Response to COVID Group, COVID Clinicians, COVID-STORM Clinicians, Imagine COVID Group, French COVID Cohort Study Group, Milieu Intérieur Consortium, CoV-Contact Cohort, Amsterdam UMC Covid-19 Biobank, COVID Human Genetic Effort, J. S. Tsang, R. Goldbach-Mansky, K. Kisand, M. S. Lionakis, A. Puel, S.-Y. Zhang, S. M. Holland, G. Gorochov, E. Jouanguy, C. M. Rice, A. Cobat, L. D. Notarangelo, L. Abel, H. C. Su, J.-L. Casanova, Autoantibodies against type I IFNs in patients with life-threatening COVID-19. *Science* **370**, eabd4585 (2020).
72. P. Bastard, E. Michailidis, H.-H. Hoffmann, M. Chbihi, T. L. Voyer, J. Rosain, Q. Philippot, Y. Seeleuthner, A. Gervais, M. Materna, P. M. N. de Oliveira, M. de Lourdes S Maia, A. P. D. A. Bom, T. Azamor, D. A. da Conceição, E. Goudouris, A. Homma, G. Slesak, J. Schäfer, B. Pulendran, J. D. Miller, R. Huits, R. Yang, L. B. Rosen, L. Bizien, L. Lorenzo, M. Chrabieh, L. V. Erazo, F. Rozenberg, M. M. Jeljeli, V. Béziat, S. M. Holland, A. Cobat, L. D. Notarangelo, H. C. Su, R. Ahmed, A. Puel, S.-Y. Zhang, L. Abel, S. J. Seligman, Q. Zhang, M. R. M. Donald, E. Jouanguy, C. M. Rice, J.-L. Casanova, Auto-antibodies to type I IFNs can underlie adverse reactions to yellow fever live attenuated vaccine. *J. Exp. Med.* **218**, (2021).
73. Q. Zhang, A. Pizzorno, L. Miorin, P. Bastard, A. Gervais, T. L. Voyer, L. Bizien, J. Manry, J. Rosain, Q. Philippot, K. Goavec, B. Padey, A. Cupic, E. Laurent, K. Saker, M. Vanker, K. Särekannu, COVID Human Genetic Effort, Etablissement Français du Sang Study Group, Constances Cohort, 3C-Dijon Study, Cerba HealthCare Group, Lyon Antigrippe Working Group, REIPI INF Working Group, T. García-Salum, M. Ferres, N. L. Corre, J. Sánchez-Céspedes, M. Balsera-Manzanero, J. Carratala, P. Retamar-Gentil, G. Abelenda-Alonso, A. Valiente, P. Tiberghien, M. Zins, S. Debette, I. Meyts, F. Haerynck, R. Castagnoli, L. D. Notarangelo, L. I. Gonzalez-Granado, N. Dominguez-Pinilla, E. Andreakos, V. Triantafyllia, C. Rodríguez-Gallego, J. Solé-Violán, J. J. Ruiz-Hernandez, F. R. de Castro, J. Ferreres, M. Briones, J. Wauters, L. Vanderbeke, S. Feys, C.-Y. Kuo, W.-T. Lei, C.-L. Ku, G. Tal, A. Etzioni, S. Hanna, T. Fournet, J.-S. Casalegno, G. Queromes, L. Argaud, E. Javouhey, M. Rosa-Calatrava, E. Cordero, T. Aydillo, R. A. Medina, K. Kisand, A. Puel, E. Jouanguy, L. Abel, A. Cobat, S. Trouillet-Assant, A. García-Sastre, J.-L. Casanova, Autoantibodies against type I IFNs in patients with critical influenza pneumonia. *J. Exp. Med.* **219**, e20220514 (2022).
74. A. Gervais, F. Rovida, M. A. Avanzini, S. Croce, A. Marchal, S. C. Lin, A. Ferrari, C. W. Thorball, O. Constant, T. Le Voyer, Q. Philippot, J. Rosain, M. Angelini, M. Perez Lorenzo, L. Bizien, C. Achille, F. Trespidi, E. Burdino, I. Cassaniti, D. Lilleri, C. Fornara, J. C. Sammartino, D. Cereda, C. Marrocu, A. Piralla, C. Valsecchi, S. Ricagno, P. Cogo, O. Neth, I. Marin-Cruz, M. Pacenti, A. Sinigaglia, M. Trevisan, A. Volpe, A. Marzollo, F. Conti, T. Lazzarotto, A. Pession, P. Viale, J. Fellay, S. Ghirardello, M. Aubart, V. Ghisetti, A. Aiuti, E. Jouanguy, P. Bastard, E. Percivalle, F. Baldanti, A. Puel, M. R. MacDonald, C. M. Rice, G. Rossini, K. O. Murray, Y. Simonin, A. Nagy, L. Barzon, L. Abel, M. S. Diamond, A. Cobat, S. Y. Zhang, J. L. Casanova, A. Borghesi, Autoantibodies neutralizing type I IFNs underlie West Nile virus encephalitis in approximately 40% of patients. *J. Exp. Med.* **220**, e20230661 (2023).
75. K. Sacco, R. Castagnoli, S. Vakkilainen, C. Liu, O. M. Delmonte, C. Oguz, I. M. Kaplan, S. Alehashemi, P. D. Burbelo, F. Bhuyan, A. A. de Jesus, K. Dobbs, L. B. Rosen, A. Cheng, E. Shaw, M. S. Vakkilainen, F. Pala, J. Lack, Y. Zhang, D. L. Fink, V. Oikonomou, A. L. Snow, C. L. Dalgard, J. Chen, B. A. Sellers, G. A. M. Sanchez, K. Barron, E. Rey-Jurado, C. Vial, M. C. Poli, A. Licari, D. Montagna, G. L. Marseglia, F. Licciardi, U. Ramenghi, V. Discepolo, A. L. Vecchio, A. Guarino, E. M. Eisenstein, L. Imberti, A. Sottini, A. Biondi, S. Mato, D. Gerstbacher, M. Truong, M. A. Stack, M. Magliocco, M. Bosticardo, T. Kawai, J. J. Danielson, T. Hulett, M. Askenazi, S. Hu, NIAID Immune Response to COVID Group, Chile MIS-C Group, Pavia Pediatric COVID-19 Group, J. I. Cohen, H. C. Su, D. B. Kuhns, M. S. Lionakis, T. M. Snyder, S. M. Holland, R. Goldbach-Mansky, J. S. Tsang, L. D. Notarangelo, Immunopathological signatures in multisystem inflammatory syndrome in children and pediatric COVID-19. *Nat. Med.* **28**, 1050–1062 (2022).
76. M. S. Abers, O. M. Delmonte, E. E. Ricotta, J. Fintzi, D. L. Fink, A. A. A. de Jesus, K. A. Zarember, S. Alehashemi, V. Oikonomou, J. V. Desai, S. W. Canna, B. Shakoory, K. Dobbs, L. Imberti, A. Sottini, E. Quiros-Roldan, F. Castelli, C. Rossi, D. Brugnoni, A. Biondi, L. R. Bettini, M. D'Angio', P. Bonfanti, R. Castagnoli, D. Montagna, A. Licari, G. L. Marseglia, E. F. Gliniewicz, E. Shaw, D. E. Kahle, A. T. Rastegar, M. Stack, K. Myint-Hpu, S. L. Levinson, M. J. Di Nubile, D. W. Chertow, P. D. Burbelo, J. I. Cohen, K. R. Calvo, J. S. Tsang, NIAID COVID-19 Consortium, H. C. Su, J. I. Gallin, D. B. Kuhns, R. Goldbach-Mansky, M. S. Lionakis, L. D. Notarangelo, An immune-based biomarker signature is associated with mortality in COVID-19 patients. *JCI Insight* **6**, e144455 (2021).
77. E. R. Shaw, L. B. Rosen, L. Ding, S. M. Holland, H. C. Su, Detection of neutralizing anti-type 1 interferon autoantibodies. *Curr. Protoc.* **2**, e511 (2022).
78. M. Vanker, K. Sarekannu, A. Fekkar, S. E. Jorgensen, L. Haljasmagi, A. Kallaste, K. Kisand, M. Lember, P. Peterson, M. Menon, T. Hussell, S. Knight, J. Moore-Stanley, P. Bastard, S. Y. Zhang, T. H. Mogensen, Q. Philippot, Q. Zhang, A. Puel, J. L. Casanova, K. Kisand, Autoantibodies neutralizing type III interferons are uncommon in patients with severe coronavirus disease 2019 pneumonia. *J. Interferon Cytokine Res.* **43**, 379–393 (2023).
79. F. Wang, J. Flanagan, N. Su, L. C. Wang, S. Bui, A. Nielson, X. Wu, H. T. Vo, X. J. Ma, Y. Luo, RNAscope: A novel in situ RNA analysis platform for formalin-fixed, paraffin-embedded tissues. *J. Mol. Diagn.* **14**, 22–29 (2012).

80. C. Liu, A. J. Martins, W. W. Lau, N. Rachmaninoff, J. Chen, L. Imberti, D. Mostaghimi, D. L. Fink, P. D. Burbelo, K. Dobbs, O. M. Delmonte, N. Bansal, L. Failla, A. Sottini, E. Quiros-Roldan, K. L. Han, B. A. Sellers, F. Cheung, R. Sparks, T.-W. Chun, S. Moir, M. S. Lionakis, NIAID COVID Consortium, COVID Clinicians, C. Rossi, H. C. Su, D. B. Kuhns, J. I. Cohen, L. D. Notarangelo, J. S. Tsang, Time-resolved systems immunology reveals a late juncture linked to fatal COVID-19. *Cell* **184**, 1836–1857.e22 (2021).
81. T. Stuart, A. Butler, P. Hoffman, C. Hafemeister, E. Papalexi, W. M. Mauck III, Y. Hao, M. Stoeckius, P. Smibert, R. Satija, Comprehensive integration of single-cell data. *Cell* **177**, 1888–1902.e21 (2019).
82. M. P. Mule, A. J. Martins, J. S. Tsang, Normalizing and denoising protein expression data from droplet-based single cell profiling. *Nat. Commun.* **13**, 2099 (2022).
83. "Annotation algorithm" (10X Genomics); https://support.10xgenomics.com/single-cell-vdj/software/pipelines/latest/algorithms/annotation.

**Acknowledgments:** We offer special thanks to J. Lack and W. Cao from the NIAID Collaborative Bioinformatics Resource team and the Genome Research Integration Team, including D. Veltri, S. Xirasagar, E Karlins, X. Cheng, J. Barnett, N. Vlasenko, K. Huang, R. Gilmore, S. Ranganathan, E. Tran, A. Yun, J. Mackey, S. Yazhuk, S. Samuel, Y. Fan, C. Shyu, J. Abrudan, C. Afrasiabi, Z. Li, L. Zhang, M. Sharma, K. Kaladi, G. Borjas, A. Elhassan, L. Myers, and J. Berghout; and to H. Orellana, S. Byers, E. Damskey, and S. Srinivasan from the NIAID Centralized Sequencing Program. We would also like to express our deep gratitude to all the individuals and families who volunteered to be part of this research. We acknowledge the sequencing services and professional partnership from the Center for Inherited Disease Research, Human Genome Sequencing Center. **Funding:** This work was supported by the Division of Intramural Research, National Institute of Allergy and Infectious Diseases, National Institutes of Health (grant AI001222 to L.D.N.and grant 1ZIAAI001059 to H.C.S.), the Estonian Research Council (grant PRG1117 to K.K.), the National Recovery and Resilience Plan (PNRR; grant MR1-2022-12376594 to C. Cifaldi), and the National Institute of Allergy and Infectious Diseases (grant 1R01AI153830-01A1 to J.E.W. and grants R01AI148963 and R01AI150300 to D.B.). **Author contributions:** Conceptualization: M.B., O.M.D., L.D.N., A.J.M., and J.S.T. Methodology: M.B., K.D., A.J.M., F.P., T.K., H.K., G.M., L.B.R., Y.Y., Y.N.L., C.L., D.F., V.O., E.S., M.S.L., A. Klion, C.O., D.B., K.K., J.S.T., D.K., S.D.R., and S. Pittaluga. Investigation: M.B., K.D., A.J.M., F.P., T.K., H.K., G.M., L.B.R., Y.Y., H.-H.Y., E.C., Y.N.L., C.L., J.S., J.N., D.F., R.C., M.R., A.C., D.R., V.O., E.S., L.H., J.K., M.S.L., M.B.S., Centralized Sequencing Program Group, M.A.W., A. Klion, C.O., K.K., J.S.T., D.K., S.D.R., and S. Pittaluga. Formal analysis: C.O., A.J.M., M.B., and L.D.N. Resources: B.B., S.K., W.A.-H., C. Cancrini, C. Cifaldi, S.B., S.S., C.S., A.R.G., A.F.F., R.S., S.C., S.C.G., T.G., D. Drozdov, I.M., D.M., B.N., R.S.A., A.E.-M., M.K., A. King, F. Licciardi, M.E.C.-M., P.P., C.P., M. Adeli, M. Algeri, F.J.A., P.B., J.R.E.B., C.B., A.B., S.O.B., M.J.B., N. Padem, M.T.d.l.M., G.D., S.S.d.R., D. Dimitrova, R.D., M.B.D., C.M.D., R.E., F.F., R.L.F., R.S.G., L.I.G.-G., H.A., A.H., A.M.H., W.I., B.K., N.K., E.K.-A., J.K., M.D.K., B.J.D.S., A. Kiykim, T.W.K., E.E.K., E.A.L., J.W.L., F. Locatelli, G.A.-L., C.M., F.C., M.M., A.O., N. Parvaneh, S. Pasic, A.P., K.P., S. Prockop, I.S.S., E.E.S., T.T., J.V., J.E.W., B.W., E.L.W., D. Draper, K.M.-H., P.M.T., S.M.H., H.C.S., and A.V. Visualization: M.B., O.M.D., A.J.M., F.P., R.C., and S. Pittaluga. Funding acquisition: K.K. and L.D.N. Supervision: L.D.N. Writing—original draft: M.B., O.M.D., A.J.M., L.B.R., D.R., V.O., D. Dimitrova, M.S.L., M.A.W., A. Klion, C.O., H.C.S., J.S.T., S. Pittaluga, and L.D.N. Writing—review and editing: M.B., O.M.D., and L.D.N. **Competing interests:** M.J.B. is a speaker for Grifols; consults for Pharming, Horizon/Amgen, and Grifols; receives sponsored research funding from the NIH, the Bill and Melinda Gates Foundation, and Pharming; and serves on the scientific advisory board for ADMA Biologics. H.C.S. has stock holdings in Amgen and Eli Lily. R.S.A. receives royalties from Elsevier for book publications, serves as deputy editor for the *Journal of Immunology*, is Committee Chair of Newborn Screening for SCID for the Clinical and Laboratory Standards Institute, and is a member of the Immunology Clinical Domain Working Group for ClinGen. B.J.D.S. is an ad hoc consultant for Sobi and a member of the Data Safety Monitoring Board for Orchard Therapeutics. I.M. is a senior Clinical Researcher at the FWO Flanders. R.L.F. has consulted for Takeda, Griffons, Horizon, and Pharming. B.W. serves as consultant for the Immunology Speakers Bureau, Takeda Pharmaceutocals. S. Prockop receives support for the conduct of clinical trials through Boston Children's Hospital from AlloVir, Atara, and Jasper. She is an inventor of intellectual property related to development of third-party virus-specific T cells program with all rights assigned to Memorial Sloan Kettering Cancer Center; receives honoraria from Pierre Fabre, Regeneron; serves on the data safety monitoring board at Stanford University and New York Blood Center; and is consulting for Atara, Ensoma, Pierre Fabre, HEOR and VOR. J.S.T. serves on the scientific advisory board of CytoReason Inc. and Immunoscape Inc. and as the co–chief science officer (unpaid) of the Human Immunome Project (nonprofit). All other authors declare that they have no competing interests. **Data and materials availability:** CITE-seq data and code are available on GEO database (accession number: GSE274284), and SomaLogic proteomics data are available on Dryad (https://doi.org/10.5061/dryad.cfxpnvxg3). All other data are available in the main text or the Supplementary Materials.

The individuals in the Centralized Sequencing Program Group include Rajarshi Ghosh, Bryce Siefert, Mari Tokita, Jia Yan, Colleen Jodarski, Mike Kamen, Rachel Gore, Nadjalisse Reynolds-Lallement, Katie Lewis, Sarah Bannon, Adrienne Borges, Nicole Gentile. Division of Intramural Research, National Institute of Allergy and Infectious Diseases, National Institutes of Health, Bethesda, MD, USA.

Submitted 30 April 2024
Accepted 12 December 2024
Published 10 January 2025
10.1126/sciimmunol.adq1697

Science Immunology

# Multiomics dissection of human RAG deficiency reveals distinctive patterns of immune dysregulation but a common inflammatory signature

Marita Bosticardo, Kerry Dobbs, Ottavia M. Delmonte, Andrew J. Martins, Francesca Pala, Tomoki Kawai, Heather Kenney, Gloria Magro, Lindsey B. Rosen, Yasuhiro Yamazaki, Hsin-Hui Yu, Enrica Calzoni, Yu Nee Lee, Can Liu, Jennifer Stoddard, Julie Niemela, Danielle Fink, Riccardo Castagnoli, Meredith Ramba, Aristine Cheng, Deanna Riley, Vasileios Oikonomou, Elana Shaw, Brahim Belaid, Sevgi Keles, Waleed Al-Herz, Caterina Cancrini, Cristina Cifaldi, Safa Baris, Svetlana Sharapova, Catharina Schuetz, Andrew R. Gennery, Alexandra F. Freeman, Raz Somech, Sharon Choo, Silvia C. Giliani, Tayfun Güngör, Daniel Drozdov, Isabelle Meyts, Despina Moshous, Benedicte Neven, Roshini S. Abraham, Aisha El-Marsafy, Maria Kanariou, Alejandra King, Francesco Licciardi, Mario E. Cruz-Muñoz, Paolo Palma, Cecilia Poli, Mehdi Adeli, Mattia Algeri, Fayhan J. Alroqi, Paul Bastard, Jenna R. E. Bergerson, Claire Booth, Ana Brett, Siobhan O. Burns, Manish J. Butte, Nurcicek Padem, M. Teresa de la Morena, Ghassan Dbaibo, Suk See de Ravin, Dimana Dimitrova, Reda Djidjik, Mayra B. Dorna, Cullen M. Dutmer, Reem Elfeky, Fabio Facchetti, Ramsay L. Fuleihan, Raif S. Geha, Luis I. Gonzalez-Granado, Liis Haljasmägi, Hanadys Ale, Anthony Hayward, Anna M. Hifanova, Winnie Ip, Blanka Kaplan, Neena Kapoor, Elif Karakoc-Aydiner, Jaanika Kärner, Michael D. Keller, Blachy J. Dávila Saldaña, Ayça Kiykim, Taco W. Kuijpers, Elena E. Kuznetsova, Elena A. Latysheva, Jennifer W. Leiding, Franco Locatelli, Guisela Alva-Lozada, Christine McCusker, Fatih Celmeli, Megan Morsheimer, Ahmet Ozen, Nima Parvaneh, Srdjan Pasic, Alessandro Plebani, Kahn Preece, Susan Prockop, Inga S. Sakovich, Elena E. Starkova, Troy Torgerson, James Verbsky, Jolan E. Walter, Brant Ward, Elizabeth L. Wisner, Deborah Draper, Katherine Myint-Hpu, Pooi M. Truong, Michail S. Lionakis, Morgan B. Similuk, Centralized Sequencing Program Group, Magdalena A. Walkiewicz, Amy Klion, Steven M. Holland, Cihan Oguz, Dusan Bogunovic, Kai Kisand, Helen C. Su, John S. Tsang, Douglas Kuhns, Anna Villa, Sergio D. Rosenzweig, Stefania Pittaluga, Luigi D. Notarangelo, Rajarshi Ghosh, Bryce Siefert, Mari Tokita, Jia Yan, Colleen Jodarski, Mike Kamen, Rachel Gore, Nadjalisse Reynolds-Lallement, Katie Lewis, Sarah Bannon, Adrienne Borges, and Nicole Gentile

*Sci. Immunol.* **10** (103), eadq1697. DOI: 10.1126/sciimmunol.adq1697

**Editor's summary**

Recombination-activating gene 1 (RAG1) and RAG2 are required for V(D)J recombination, which directs mature B and T cell development and a fully functional adaptive immune system. Hypomorphic variants of the *RAG* genes in humans results in an array of immunodeficiencies, which all have distinct features for reasons not well understood. Bosticardo *et al.* performed a multiomics analysis of 157 patients with RAG deficiency who presented with a spectrum of disease phenotypes along with 135 age-matched controls. Analyzing blood, bone marrow, and other tissue biopsies, the authors found prominent signatures of immune dysregulation with both common and distinctive features in these patients. These findings may direct phenotype-specific therapeutic interventions before patients can receive definitive treatments. —Seth Thomas Scanlon